A multi-proxy study of a Holocene peat sequence on Nightingale Island, South Atlantic

Hanna Lindvall

Masters thesis in Geology at Lund University,
no. 276
(45 hskp/ECTS)

Department of Earth- and Ecosystem Sciences
Division of Geology
Lund University
2011

A multi-proxy study of a Holocene peat sequence on Nightingale Island, South Atlantic

Master Thesis
Hanna Lindvall

Department of Earth and Ecosystem Sciences
Division of Geology
Lund University
2011

Contents

Cover Picture: Islets of Nightingale Island. Photo: Svante Björck.

A multi-proxy study of a Holocene peat sequence on Nightingale Island, South Atlantic

HANNA LINDVALL

Lindvall, H., 2011: A multi-proxy study of a Holocene peat sequence on Nightingale Island, South Atlantic. *Examensarbeten i geologi vid Lunds universitet*, No. 276, 32 pp. 45 ECTS credits.

Abstract: Nightingale Island is situated at 37°S in the central part of the South Atlantic Ocean, which is a sensitive location for variations within the Atlantic Meridional Overturning Circulation (AMOC) and the Southern Hemisphere Westerlies (SHW) wind belt. A peat sequence from the wetland 2nd Pond has been investigated with emphasis on the composition of the deposits, loss on ignition (LOI), total Carbon (TC), Nitrogen (N), biogenic Silica (BSi), magnetic susceptibility (MS), diatom counting and macrofossil analysis. The proxies reveal a pattern of recurring cycles of short oscillations lasting between 200 and 2000 years. The oscillations are clearly seen by increased MS and decreased TC, N and LOI values. An age-model based on radiocarbon dating gives detailed information about the timing of the oscillations. The study also compares these results with a previous study from the same wetland. Ljung and Björck (2007) did similar investigations and found a pattern of fairly short oscillations, which they interpreted as periods with increased precipitation. The changing pollen assemblages were important for this conclusion. The oscillations are in general well correlated between the two sites within the wetland, but with some differences. These are mainly due to the exact timing of events and can mostly be explained by uncertainties within the age-models. The main forcing factors behind these precipitation-rich oscillations are thought to be changes of the position of SHW or increased SST (sea surface temperature) in the central South Atlantic Ocean. Increased SST may be due to a weaker AMOC and an interglacial bipolar seesaw might be in action although more studies are needed to confirm or reject the hypothesis. A short literature review of South American Holocene climate reconstructions reveals a very diffuse record. Many signs of climate change are found but few of them are consistent and synchronized between different sites, although geographical differences may be part of the explanation.

Keywords: Nightingale Island, South Atlantic, Holocene, peat, C/N, environmental reconstruction, interglacial bipolar see-saw.

Hanna Lindvall, Department of Earth and Ecosystem Sciences, Division of Geology, GeoBiosphere Science Center, Lund University, Sölvegatan 12, SE-223 62 Lund, Sweden. E-mail: Hanna@skposeidon.se

Studier av en holocen torvlagerföljd på Nightingale Island i Sydatlanten

HANNA LINDVALL

Lindvall, H., 2011: A multi-proxy study of a Holocene peat sequence on Nightingale Island, South Atlantic. *Examensarbeten i geologi vid Lunds universitet*, Nr. 276, 32 s. 45 hp.

Sammanfattning: Nightingale Island är belägen på 37°S i den centrala delen av Sydatlanten. Dess geografiska position är känslig för variationer av den termohalina circulationen i Atlanten och för förändringar av västvindsbältet på södra hemisfären. En lagerföljd från ett litet kärr, 2nd Pond, på ön har undersökts med avseende på sediment-typ, glödförlust, kol-, kväve- och kiselhalt, magnetisk susceptibilitet, diatomékoncentration och makrofossilinnehåll. Tillsammans avslöjar analyserna ett mönster av återkommande perioder, 200-2000 år långa, med klimatförändringar. Perioderna ses tydligt i analysresultaten genom ökad magnetisk susceptibilitet och minskad mängd organiskt material, kol och kväve i avlagringarna. En åldersmodell baserad på ^{14}C-dateringar används för att datera perioderna med klimatsvängningar. I studien jämförs resultaten med en tidigare studie av Ljung och Björck (2007). Även i den studien har man noterat återkommande perioder med ändrade analysvärden och under klimatsvängningarna förändras dessutom pollensammansättningen i kärret. Det har tolkats som att ökad erosion för med sig mer pollen från växter längre bort i avrinningsområdet. De båda studierna stämmer generellt väl överens och skillnaderna, som huvudsakligen rör den exakta dateringen av de fuktiga perioderna, är troligen mestadels orsakade av osäkerheten i åldersmodellerna.

De styrande faktorerna som orsakar de korta klimatsvängningarna med ökad nederbörd och erosion tros vara förändringar av västvindsbältets intensitet och spatiala utbredning, eller havstemperatur-förändringar i södra Atlanten. Det sistnämnda kan hänga ihop med den termohalina circulationen och ett motverkande klimat-samband (en s.k. gungbrädeseffekt) kan finnas mellan norra och södra Atlanten. När det blir kallt i Nordatlanten tycks det samtidigt bli varmt i Sydatlanten och vice versa, men för att bekräfta hypotesen krävs fler undersökningar. En mindre litteraturstudie av undersökningar som fokuserar på klimatförändringar i Sydamerika under holocen visar ett brokigt mönster. Många olika tecken på klimatförändringar och kortare klimatfluktuationer finns, men data från olika platser stämmer sällan överens. De olika geografiska lägena där undersökningarna utförts kan till viss del förklara det, men mer forskning krävs innan vi förstår klimatvariationerna i Sydatlanten bättre.

Nyckelord: Nightingale Island, Sydatlanten, Holocen, torv, C/N, miljörekonstruktion, interglacial gungbrädeseffekt.

Hanna Lindvall, Institutionen för geo– och ekosystemvetenskaper, Enheten för Geologi, Centrum för GeoBiosfärsvetenskap, Lunds Universitet, Sölvegatan 12, 223 62 Lund, Sverige. E-post: Hanna@skposeidon.se

Studier av en holocen torvlagerföljd på Nightingale Island i Sydatlanten

HANNA LINDVALL

Lindvall, H., 2011: A multi-proxy study of a Holocene peat sequence on Nightingale Island, South Atlantic. *Examensarbeten i geologi vid Lunds universitet*, Nr. 276, 32 s. 45 hp.

Populärvetenskaplig sammanfattning: Vi människor och vårt samhälle påverkas mycket av klimatet vi lever i och av de naturliga klimat- och miljövariationer som sker på jorden. Det kan vara kortvariga katastrofartade händelser som tsunamis och jordbävningar men också långsammare och långvariga klimatförändringar som påverkar vårt sätt att leva och bruka jorden. Genom geologiska studier av jordens historia vet vi att klimatet har varierat mycket ända sedan jorden bildades för 4.55 miljarder år sedan. Storskaliga förändringar beror till exempel på att jordens bana runt solen inte är helt rund och likformig över tid samt att solaktiviteten varierar. Men många andra faktorer påverkar också och om många av dem vet vi ännu inte så mycket. Genom forskning som syftar till djupare kunskap om hur jordens klimat varierat försöker vi förstå mekanismerna som orsakar förändringar. Genom ökad kunskap om tidigare förändringar hoppas vi kunna förutse och förbereda oss bättre inför framtida klimatförändringar.

I den här studien har ett litet kärr på Nightingale Island i Sydatlanten undersökts. En torvsekvens som täcker de senaste 10000 åren har analyserats med flera olika metoder. Resultatet tyder på att stora förändringar har skett. Under flera korta perioder blir klimatet enligt mina tolkningar av data plötsligt fuktigare och eventuellt varmare. Därefter sker en snabb återgång till ett torrare klimat igen innan ännu en fuktig period plötsligt inleds. Perioderna är mellan 200 och 2000 år långa. Eftersom Nightingale Island ligger mitt ute i Atlanten påverkas ön mycket av oceanströmmarna och av det s.k. västvindsbältet som är ett brett band av vindar som blåser från väst till öst på mellanlatituderna. Förändringar i havsströmmarna och västvindarna runt Nightingale Island kan bero på stora förändringar som kanske påverkar hela södra hemisfären eller t.o.m. hela jordklotet. Genom studien på Nightingale Island ökar förståelsen för vilken typ av förändringar som skett de senaste 10000 åren. Om man kartlägger vilka processer och faktorer som varit drivande i förändringarna kan man förstå dynamiken i klimatförändringarna bättre.

I studien undersöktes avlagringarna i kärret, vilka mestadels utgörs av välnedbruten torv, och deras innehåll av kisel, kol, kväve och organiskt material bestämdes. Dessutom analyserades de med avseende på magnetisk susceptibilitet, vilken i denna typ av vulkanisk miljö visar hur halten av minerogena partiklar varierar. Under de fuktiga perioderna har det regnat mer, och då har minerogena partiklar från omgivningen runt kärret eroderats mer effektivt. De fuktiga perioderna kan därför tydligt ses i resultaten som perioder med lägre organisk halt och högre magnetiska värden till följd av det mer minerogena materialet som tillförts kärret.

Resultaten har även jämförts med en tidigare studie från samma kärr och de två undersökningarna stämmer väl överens. Även från andra områden på södra halvklotet finns många olika indikationer på att klimatet varierat mycket de senaste 10000 åren, men hittills vet vi inte exakt när olika förändringar skett och vilka processer som har orsakat dem. Därför behövs ännu mer forskning inom området.

Hanna Lindvall, Institutionen för geo– och ekosystemvetenskaper, Enheten för Geologi, Centrum för GeoBiosfärsvetenskap, Lunds Universitet, Sölvegatan 12, 223 62 Lund, Sverige. E-post: Hanna@skposeidon.se

1 Introduction

1.1 Aim and background

Mankind strives to gain knowledge; about herself, the society and the Earth, and about the present, past and - above anything else - the future. The future climate is an essential question mark since it may affect individuals, society and the Earth. Driving and forcing mechanisms of the climate system are complex and still today not fully understood. Through monitoring the present climate, and studying and analysing past climate changes, we try to project future climate scenarios and their potential challenges for mankind.

The last ice age lasted 115.000-11.700 calendar years before present (cal. BP) (Robinson *et al.* 2010; Rasmussen *et al.* 2006). Large inland ice-sheets covered much of Scandinavia, Russia and North America. Global sea level was more than 100 meters lower than today and the climate, although variable, was essentially colder and harsher. At the last glacial termination the inland ice-sheets melted, temperature and sea-level rose, massive icebergs were discharged into the Atlantic Ocean and changes in the global ocean circulation occurred.

The ongoing interglacial, the Holocene, displays a more stable climate with changes of smaller amplitude. But even during the Holocene several important regional climate fluctuations have occurred, such as the Holocene Thermal Optimum and the 8.2 ka event in the Northern Hemisphere (NH). The climate development is rather well monitored in the NH where much research has been performed and where many climate archives, such as lake and marine sediments, are easy to access. Accumulated lake sediment and peat sequences offer high-resolution paleoenvironmental records and permit detailed reconstructions of the climate development.

In the Southern Hemisphere (SH), however, much less is known about the Holocene climate fluctuations. Due to fewer suitable archives and the economical and logistic aspects of reaching climate archives at good sites, less research has focused on climate change in the SH. The extensive oceans offer deep sea sediments as climate archives but the sedimentation rate is usually very low and the records therefore have low temporal resolution, which is inappropriate when interpreting short-lasting changes (centennial to millennial scale).

Fig. 1. Map of the South Atlantic Ocean. The position of the Tristan da Cunha archipelago is indicated by the arrow.

Oceans are clearly one of the main features of Earth's climate system. With increased knowledge about climate changes in the central South Atlantic Ocean since the last glacial termination we will gain a better understanding of global climate dynamics. Analysing sediment sequences from different locations is a good method to increase the understanding of the climate system. The Tristan da Cunha island group, situated in the central South Atlantic Ocean, has a very strategic position for such studies (Fig. 1).

1.2 Project idea

The main aim of this thesis is to investigate and interpret a peat record from the site 2nd Pond on Nightingale Island, Tristan da Cunha island group, in terms of paleoenvironment and paleoclimate. This is done by multi-proxy analyses of a core from the littoral part of this wetland. The methods used are core examination and description, loss on ignition, biogenic silica, diatom concentration counting, magnetic susceptibility, microscope- and macrofossil analysis and carbon- and nitrogen analysis. Radiocarbon dating is used to obtain a reliable chronology for the sequence. The main idea of this thesis is to test a hypothesis put forward by Ljung and Björck (2007) in connection with the former's PhD thesis (Ljung 2007). Ljung and Björck (2007) based their interpretations on data from the same wetland, but from a core in the central part of the basin. The hypothesis put forward is that hydrological changes, i.e. more or less precipitation, are responsible for a series of recurrent Holocene changes in sedimentology, magnetic susceptibility, geochemistry and pollen assemblages. As far as possible, the results will also be placed into a wider paleoclimatic perspective. Literature studies are important to reach this aim.

1.3 Study area

The Tristan da Cunha island group consists of three small islands and some even smaller islets at 37°S, 12°W in the central part of the South Atlantic Ocean (Fig. 1). The islands were discovered by Portuguese explorers in 1506 (Ryan 2007) and have thus not been subject to human disturbances prior to that date.

The archipelago is located at a volcanic hotspot and thus formed by volcanic activity. Nightingale may be up to 18 Ma old and the most recent volcanic activity on the island is dated to >200.000 years ago (Ryan 2007). There are, however, indications of much younger volcanic activity (S. Björck personal communication 2011). The most recent volcanic activity in

the area is the eruption on Tristan da Cunha Island in 1961 and a submarine eruption offshore Nightingale in 2004 (Reagan *et al.* 2008). Some lower parts of the island are made up by pyroclastic deposits, while trachyte covers the main and high areas, e.g. around the ponds (Fig. 2, Ryan 2007; Baker 1973). Trachyte is an extrusive, magmatic rock formed from a parent basaltic lava and the main constituting minerals are alkali feldspars (Hedin & Jansson 2007; *Encyclopædia Britannica Online 2011*). It has a porphyritic texture with phenocrysts, mainly of plagioclase (Baker 1973), but other minerals such as biotite, hornblende and pyroxene may also be present (Hedin & Jansson 2007; *Encyclopædia Britannica Online 2011*). The island is ca. four km^2 in size today, but the shallow (50 m) plateau around the island shows that it has been considerably larger, e.g. during the Last Glacial Maximum (LGM), not too long ago (cf. Ollier 1984). The highest point of Nightingale Island is 400 m a.s.l. (Ryan 2007).

The site investigated is a fen called 2nd Pond, and it is one of four wetland areas in the interior part of the island (Fig. 2 and 3). 2nd Pond is approximately 350 x 150 meters in size and the altitude is 200 m a.s.l. (S. Björck personal communication 2011). The basin has no visual in- or outflow of surface water (Ljung 2007) and the hill-sides are rather steep. Today the wetland surface is dominated by the bog grass *Scirpus* sp. (a genus of sedges) and *Sphagnum* sp. (Ljung 2007). *Spartina arundinacea*, tussock grass, dominates the surroundings of the pond as well as most of the island. The grass may be up to three meters high and grows in tussocks or dense stands (Ryan 2007). *Blechnum palmiforme* (bog fern) and *Phylica arborea* (Island tree) are bigger (up to 1.6 and 8 meters, respectively) and grow in the catchment (Ryan 2007). The island is inhabited by a huge amount of birds, mainly sea-birds, and they have a major environmental impact as they bring nutrients to the island and affect the natural vegetation by burrowing and trampling (Ryan 2007).

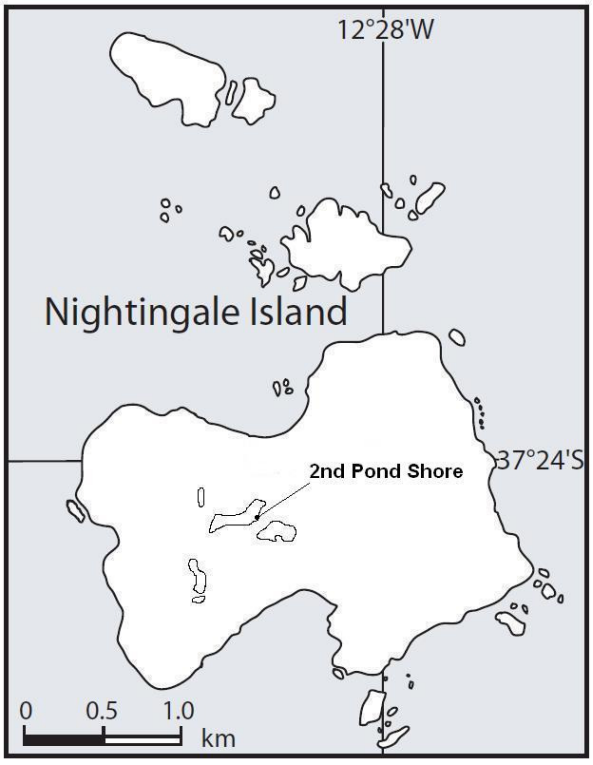

Fig. 2. Map of Nightingale Island and the Ponds. The coring site of the 2nd Pond Shore sequence is indicated.

1.4 Climate

The climate at Tristan da Cunha is moist and temperate with small annual variations. The mean annual air temperature at sea level is 14.5°C. Three important atmospheric systems affect the South Atlantic Ocean.

1. A subtropical high-pressure cell is situated around 20°S in the Atlantic Ocean. During austral summer it moves slightly southwards (Hess 2011).
2. The Southern Hemisphere westerlies (SHW) are the prominent winds blowing from west to east at the mid latitudes (30-60°S) (Fig. 4A). They are driven by the subtropical high-pressure cell since air sinks to the surface in the cell and then deflects towards the southwest of the cell. The Tristan da Cunha islands are situated in the northernmost part of the SHW and the average wind speed is 36 km/h (Ryan 2007). The wind direction at low elevations is however not always towards the east since surface processes and migratory pressure systems

Fig. 3. 2nd Pond. The arrow indicates the coring position for the peat sequence analysed in this work. Photo: Svante Björck.

influence the surface winds (Hess 2011).

3. The subtropical jet stream is a core of more consistent westerly winds meandering above the surface westerlies at around 30°S (Hess 2011).

The sea surface temperature (SST) at Tristan da Cunha is around 18°C with only minor annual variations (Ljung 2007). Oceanographically there are three main features of the South Atlantic Ocean:

1. The surface waters of the South Atlantic Ocean circulate counter-clockwise as a huge gyre (the South Atlantic gyre, see Figure 4B). The water flows southwards along the South American coast, deflects eastwards over the ocean at mid latitudes and flows northward along the African west coast. At low southern latitudes close to the equator, the water is again deflected and crosses the ocean towards South America to complete the gyre. These currents are driven mainly by the atmospheric circulation, e.g. the trade winds push the ocean surface water towards the west close to the equator and the SHW push the water towards the east in the mid latitudes. By the Coriolis effect, currents are deflected to the left in the SH, fulfilling the circular pattern of the surface currents (Hess 2011).
2. A net transport of relatively warm water flows at shallow depths from the Indian Ocean, south of Africa and into the South Atlantic Ocean where it continues into the North Atlantic Ocean (Hess 2011).
3. At depth, cold and dense water flows southward from the North Atlantic Ocean, through the South Atlantic and becomes part of the cold and salty deep waters of the Antarctic Circumpolar Current (ACC), or it continues into the Indian Ocean. The deep ocean currents' average flow speed is only 15 km/year (Hess 2011).

The mean annual precipitation at Tristan da Cunha is 1670 mm. The precipitation depends on SST, SHW and temporary cold fronts passing the area (Ljung 2007; Ryan 2007), and precipitation is higher during austral winter (Ljung 2007). There are large variations in precipitation on the Tristan da Cunha Island due to orographic (topographic) effects (Ryan 2007). No specific climate data is available from Nightingale Island but it is likely to be similar to the climate at Tristan da Cunha Island. Due to its smaller size and the lack of large topographical differences on Nightingale Island, a more even precipitation pattern is likely (Ljung 2007). The lower elevation of the island may also reduce the precipitation rates considerably compared to Tristan da Cunha (K. Ljung personal communication 2011), where the peak reaches 2060 m a.s.l. North of the islands the precipitation rates are essentially lower due to the high-pressure cell (Ljung 2007).

As indicated above, the global ocean circulation connects the different oceans and transfer climate signals to other oceans and continents. The position of Tristan da Cunha is thus thought to be very sensitive to large-scale oceanic and atmospheric circulation changes.

2 Methods

2.1 Core collection

The laboratory work is based on a sequence of almost five meters (485 cm) of deposits. The cores were collected in February 2010 with a Russian corer with a one meter long chamber (Fig. 5). The cores were collected five to ten meters from the shore of the wetland

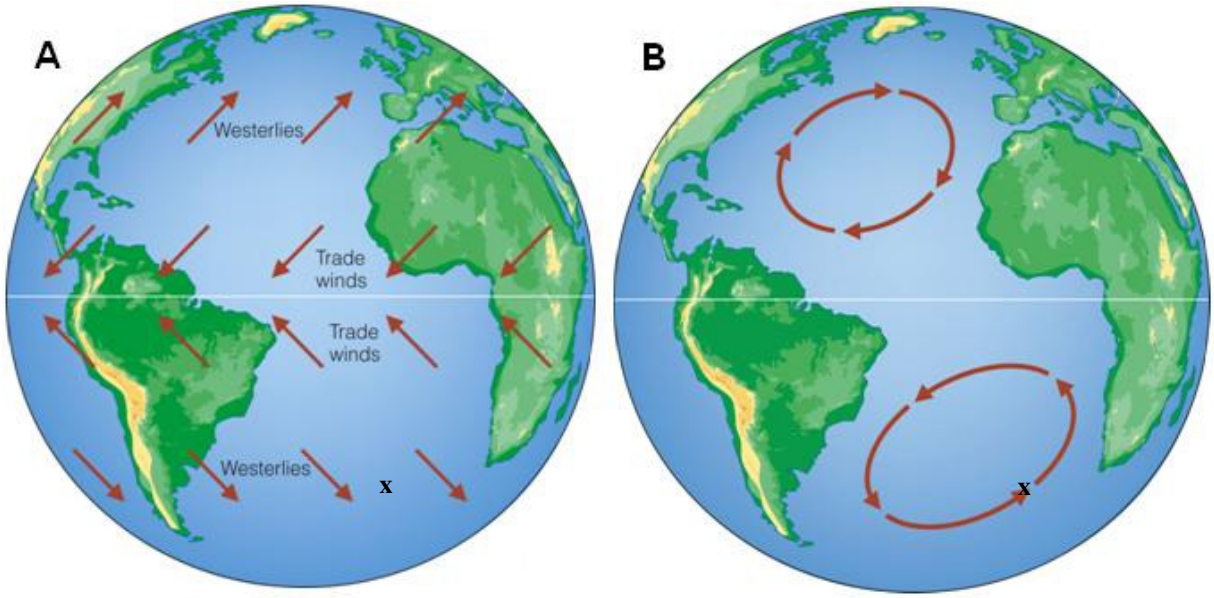

Fig. 4. Schematic map of the dominating wind belts in the Atlantic Ocean. Tristan da Cunha (indicated by x) is situated at the northern boundary of SHW (A). General map of the dominating surface currents in the North and South Atlantic Ocean (B) (Fanelli).

at the GPS position S 37° 25’ 29.4’’ W 12° 29’ 08.3’’. The cores are 7.5 cm wide, apart from the lowermost one (5 cm) and they were collected from two separate holes close-by with an overlap of about 20 cm. The coring reached to the bedrock or a stone. After transport home the cores have been stored in a cold room (+5°C).

2.2 Magnetic susceptibility

The magnetic susceptibility (MS) of the cores was measured prior to all other laboratory work. During measurement a weak magnetic impulse is induced to the core and the magnetic response is measured. A measurement is made every five mm of the core and a blank measurement is done in the air as a reference in-between every sample measurement. The obtained value is a measurement of how easily the sediment and deposits can be magnetized, which often corresponds well to the minerogenic content, which in turns depends much on the in-wash of minerogenic particles from the surroundings. Since several different types of magnetism is measured at the same time, there is a risk that mineral grains interact and gives an unrealistically low response, but this mostly has a very small influence. Post-depositional processes may also change the magnetic properties of the sediment through dissolution and authigenesis (production of new magnetic minerals) (Sandgren & Snowball 2001). The measurements were done with a Bartington Instruments Ltd MS2E1-sensor and TAMISCAN-TS1.

2.3 Core correlations

The core correlations are based on lithological changes and magnetic susceptibility. In a few cases, the magnetic susceptibility was re-measured to reach a safer base for the correlations. The methods for correlation and the overlap for every core are shown in Table 1.

2.4 Core examination and subsampling

The cores were described with respect to lithology, colour, organic material and texture. Subsampling was done throughout the whole core sequence after primary examinations. In total 102 samples of about one cm^3 were collected at every five cm on average. After four days of freeze-drying the samples were stored in a dessicator and divided for further analysis. One sample from each unit was also collected for microscope- and macrofossil analysis.

2.5 Microscopic inspection and macrofossil analysis

The deposits was inspected under light microscope. For the minerogenic-rich units the aim was to check for tephra (volcanic ash) layers and other minerogenic material. For the peat units it was primarily done to distinguish between the different lithologies, and to perform a basic macrofossil analysis. To dissolve sediment aggregates, the samples were treated with 5% sodium hydroxide (NaOH) for one to two days and then sieved prior to analysis. For the humified peat samples, a 250 µm sieve was used, and for minerogenic-rich sediment, gyttja-like fen peat and highly humified fen peat samples a 100 µm sieve was used. Species identification is generally difficult due to the special flora with many endemic plants. Attempts were focused on identifying species mentioned in the field guide by Ryan (2007), but it does not show pictures of leaves or seeds that may be found in the subsamples.

2.6 Loss on ignition

Loss on ignition (LOI) is a simple method to deter-

Fig. 5. A picture of the uppermost core, shown between 94 and 149 cm below the surface. A minerogenic horizon is visible in the middle part of the core. Photo: modified after Svante Björck.

Table 1. The overlap and correlation methods between the six different cores. The cores are counted from the bottom (core 1 is thus the lowermost one).

Cores	Overlap (cm)	Correlation method
1-2	41	Magnetic susceptibility
2-3	18	Magnetic susceptibility
3-4	16	Magnetic susceptibility
4-5	23	Magnetic susceptibility and a horizon with minerogenic-rich sediment at 365.5-366.0 cm
5-6	17	A distinct colour- and lithology change (unit 21-22)

mine the organic content of a deposit. The material is combusted in a muffle furnace where the organic matter is oxidized to CO_2 and ash. Weighing the samples before and after combustion allows calculation of the organic content. LOI was carried out as follows: cleaned crucibles were dried in an oven at 105°C overnight (>12 hours), cooled down in a dessicator and weighed. The samples (mostly 0.3-0.6 g/sample) was dried and cooled down as above before scaling. The samples were put into the muffle furnace, heated up during two hours and then combusted for four hours at a constant temperature of 550°C. The samples cooled down in a dessicator before the final weighing.

Calculation of the organic content (Heiri *et al.* 2001):
((DW before combustion – DW after combustion)/DW before combustion) x 100 = LOI (%)
DW = dry weight

Many factors influence the results when LOI is being measured, for example the sample weight, combustion time, combustion temperature and where in the oven the samples are placed. Therefore it is important to be consistent during the laboratory work and not to overinterpret minor changes (Heiri *et al*. 2001). De Vos *et al.* (2005) tested the method compared to Total Organic Carbon analysis and concluded that LOI measurements are reliable except for when organic matter (OM) content is low. A risk with using LOI as an estimate of TC is the presence of volatile inorganic components, which might result in too high LOI values (Meyers & Teranes 2001).

LOI more or less equalizes the organic content of the deposits. Typically organic matter consists of about 50% carbon, but the exact number varies (see e.g. Meyers and Teranes (2001), De Vos *et al.* (2005) and Luczak *et al.* (1997)). Calculating LOI/TC ratio allows a comparison of the results and it may add more information about the carbon compound of the deposits.

2.7 Carbon and nitrogen analysis

Analyses of the carbon (C) and nitrogen (N) content in deposits give information about two important elements in organic deposits, but also indications of the source of the deposit. Terrestrial organic matter contains a high amount of C originating from cellulose tissues. Typical C/N ratios for a terrestrial deposit are 20 or above (Meyers & Teranes 2001). Sediments mainly formed by aquatic biologic production are often dominated by algae, containing more N which originates from the lipids and proteins of the organisms (Talbot 2001). Typical values of the C/N atomic ratio in lake sediments are 4-10 (Meyers & Teranes 2001).

Prior to elemental analysis the freeze-dried samples are ground in a shaking cylinder with metal bulbs. Three mg of a sample is added into small tin capsules, which are then folded to keep it in place and to minimize the air in the sample. The samples are loaded in an auto-sampler and run through the elemental analyser. In the first step the sample enters the pre-chamber where a constant flow of helium gas keeps the air out. The sample is then dropped down into the reaction tube which keeps a temperature of 1050°C. This is a quartz tube filled with chromium oxide and silvered cobalt. Just after the sample is dropped into the hot reaction chamber a specific amount of oxygen gas (O_2), depending on the exact weight of the sample, is led into the chamber. The tin capsule and the sample are instantly and completely combusted and a temperature of 1700-1800°C are reached momentarily. Ash and gases, mainly CO_2, N_2, H_2O and SO_2, remain. Through the constant helium flow the remaining gases will be pressed through the reagents in the reaction tube, and unwanted gases such as halogens and sulphur will be trapped.

The next step is the 650°C hot reduction tube filled with small copper wires. Here any NO_x and N_2O are reduced to N_2 and any remaining O_2 is absorbed. The retained gases (CO_2, N_2 and H_2O) go through a tube filled with magnesium perchlorate to trap H_2O. CO_2 and N_2 are then pushed through a two meters chromatographic separation column with a constant temperature of 80°C. Because of the different molecule size, the N_2 gas runs faster through the column than the CO_2 gas and arrives to the thermal conductivity detector (TCD) prior to the CO_2 (Fig. 6). The TCD measures the gases as peaks of electrical force, and the area below the peak is calculated with computer software to show concrete values of the N and C contents. A calibration set with known amounts of C and N is used to calibrate the unknown samples. The analysis was conducted with a Costech Instruments ECS4010 elemental analyser and EAS32 computer software.

Results from elemental analysis are presented as total carbon, TC%, nitrogen, N%, and a quota of C/N*1.167 where 1.167 is used to compensate for the different molecule weights of C and N. The C/N ratio is thus expressed as atom ratios between the elements. The values assume that no inorganic carbon, originating from carbonate bedrock, is present (Meyers & Teranes 2001).

2.8 Biogenic silica

Analysis of the biogenic silica content of a deposit is an easy way to get important information of how the aquatic productivity in a lake has changed over time. Silica is one of the most common elements on Earth and exists in both highly resistant phases such as crystalline quartz and more easily soluble phases (dissolved silicate (DSi) and biogenic silica (BSi)). DSi is essential for aquatic organisms such as diatoms, sponges, chrysophytes and radiolarians. They collect DSi from the water and precipitate it as BSi in shells, spicules and cysts. Terrestrial plants absorb DSi from the soil and precipitate it in phytoliths in their tissues. Other forms of non-crystalline (amorphous) silica may also be present, e.g. originating from weathering or volcanic glass, but in aquatic systems these are usually

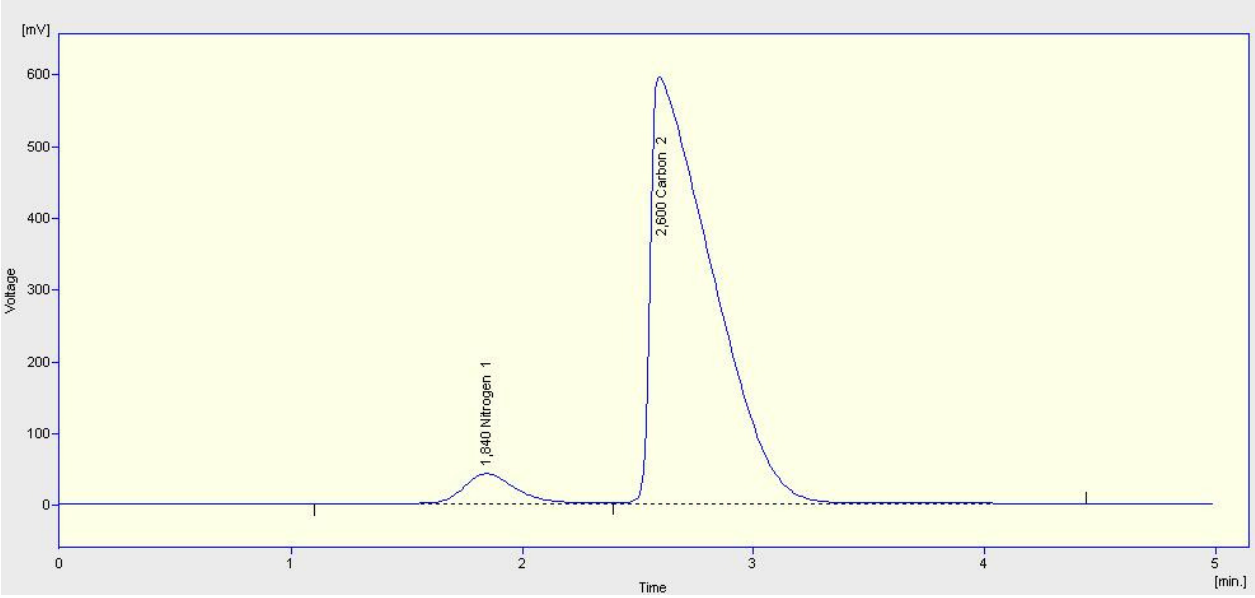

Fig. 6. A chromatogram from C/N analysis shows clearly how the N_2 gas reaches the TCD prior to the CO_2 gas. On the horizontal axis, the time is shown. The largest amount of N_2 arrives 1.84 minutes after combustion and CO_2 after 2.6 minutes. The vertical axis shows the electrical response in milli-volts (mV).

negligible. Awareness of the non-biogenic, amorphous silica and knowledge about the sediment source is important when interpreting the data.

A wet-alkaline digestion technique was used for the measurement of BSi. 30 mg of freeze-dried and homogenized samples were weighed into plastic bottles. 40 ml of a weak base solution (1% Na_2CO_3) was added to every sample. Samples were shaken at 85°C where digestion of silica occurs. This is a surface reaction where the base solution catalyses the reaction. Sub-sampling was done after three, four and five hours. The samples were removed from the warm bath and put into cold water which rapidly decreases the rate of reaction. One ml of the solution was transferred into plastic bottles with nine ml of an acid liquid (0,021N HCl) to neutralize and stop the reaction.

The sub-samples from three, four and five hours were analysed with the molybdate blue methodology: Ammonium molybdate, ascorbic acid and oxalic acid were added to the samples and run through a system calibrated with a series of standards. The ammonium molybdate reacts with the dissolved silica and the liquid turns slightly bluish. The colour is measured in a spectrophotometer and a peak is printed for every sample.

Crystalline silica and BSi react and dissolve at different rates, and through sub-sampling of the reaction at different times a linear regression is calculated, and from that the amount of BSi is determined. The easily soluble phases, which mostly originate from organic material (diatom frustules and plant tissues), are dissolved after two hours. Crystalline phases of silica take much longer to dissolve. Through calculating a linear regression between the three-, four- and five- hour values we can differentiate between the biogenic silica dissolved (the value where the linear regression crosses the vertical axis) and the dissolving crystalline silica (the slope of the linear regression) (Fig. 7). Corrections are made for the different solutions used.

The analysis was carried out using Technicon Industrial Method 186-72W-Modified on a Technican Auto Analyzer II system (Conley and Schelske 2001). In general, the analytical results are considered to be within ± 10% accuracy of the measured value.

The littoral core has been analysed throughout the sequence (102 samples) and complementary samples from a core from the central part of 2nd Pond have been analysed. These samples were chosen because they represent marked increases and decreases in diatom abundance. The question raised was whether this is notable in the biogenic silica record or not.

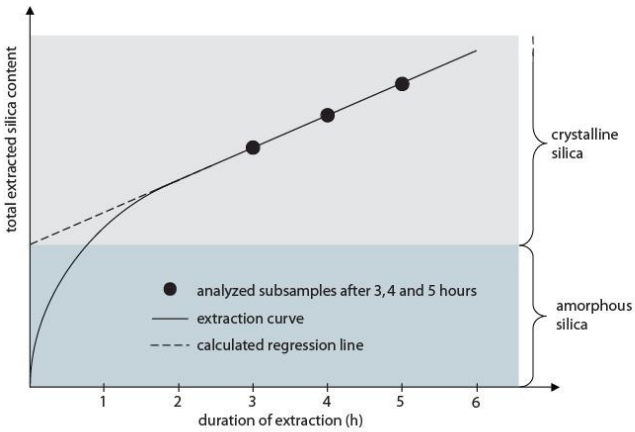

Fig. 7. A model of the extraction curve of silica, the sampling hours and the calculated regression line. Amorphous silica is easy dissolvable and usually completely extracted prior to the first subsampling. Crystalline silica dissolves at a lower velocity, and a linear regression of the extracted crystalline silica content is calculated.

2.9 Diatom concentrations

Diatoms are unicellular algae with siliceous shells (frustules). They inhabit both fresh and saline water and other damp environments, and they are sensitive to environmental conditions such as pH, temperature and nutrient status (Battarbee 2001; Lowe and Walker 1997). Diatom concentration counting has been made in a core from the central part of 2nd Pond and as a complement to this study also in four samples from the 2nd Pond Shore core (the main core of this study). The diatom concentration indicates the productivity level in the lake and is usually strongly coupled to the nutrient status.

2.10 Radiocarbon dating

Radiocarbon dating is the most widely used absolute dating method for late Quaternary sediments. ^{14}C is produced in the upper atmosphere when neutrons collide with ^{14}N and produce ^{14}C isotopes. ^{14}C, as well as the stable carbon isotopes ^{12}C and ^{13}C, is oxidized to CO_2 and then mixed in the atmosphere and oceans, and by photosynthesis taken up by organisms to the biosphere. A living organism is in balance with the isotopic ratio of $^{14}C/^{12}C$ in the atmosphere during its lifetime. When the organism dies, no more exchange with the atmosphere occurs. The ^{14}C incorporated in the dead organism decays with a half-life of about 5700 years. The activity after the decay of ^{14}C is measured with accelerator mass spectrometry (AMS) and time of death for the organism is calculated (Lowe & Walker 1997).

For radiocarbon dating, each sample is first graphitized. When run in the accelerator mass spectrometer a large potential difference makes ions (the ^{14}C ions among others) travel very fast in the spectrometer. Strong magnets and electric fields are used to deflect them from the straight path. Depending on the mass and charge of different ions, they deflect differently and it is possible to measure the amount of ^{14}C ions.

17 subsamples of bulk peat were submitted for radiocarbon dating at the SSAMS laboratory in Lund. The radiocarbon age was transferred to calendar years with the calibration curve for the southern hemisphere, SHCal04 (McCormac *et al.* 2004; Bronk Ramsey 2009). The main source of error apart from the calibration is likely to be presence of reworked organic material. Also a possible different ocean circulation particularly during the last glacial termination might have affected the ^{14}C ratios in the SH and there is a question about how accurate the SHCal04 is during parts of the last deglaciation (Lamy *et al.* 2007).

2.11 Age-depth model

An age-depth model was constructed to obtain a reliable chronology and an age of the different events in the stratigraphy. This was done with OxCal v.4.1.7 (Bronk Ramsey 2009). The Poisson process deposition model (P_sequence) is used, which takes into account the radiocarbon age with the calibration curve and the depth of each sample, thus always forcing the model to create older ages with increasing depth. The sedimentation rate range, or how fast the sedimentation rate is allowed to change, is described by the *k* parameter. $k = 0.3$ is used in this model (Bronk Ramsey 2008).

2.12 Statistical tests

Several different statistical techniques have been used to test the data quality.

The Pearson's product moment correlation is an index used to find out the strength of the relationship between two variables. E.g. to what extent do two variables, e.g. LOI and BSi, vary together? The calculated correlation coefficient will have a value between -1 and 1. 1 is a perfect linear and positive correlation, and -1 is a perfect negative correlation. An index close to zero is a very weak or non-existant relationship. By squaring the correlation coefficient a more concrete value, the coefficient of determination (R^2), is given. This gives a number of how much of the variations in one data set (one variable) is shared in common with the other variable. E.g. if the Pearson's product moment correlation is 0.7 (a strong direct relationship) the coefficient of determination will be $0.7^2 = 0.49$, or 49%. Then the two variables have 49% of their variance in common (Salkind 2008).

During analysis of TC, N and BSi standard samples are used and the regression line of best fit is calculated. A linear relationship was calculated for BSi samples, whereas a quadratic formula was used for TC and N. To estimate how well the calibration line fits to the standard samples, the coefficient of determination (R^2) is calculated. For both TC, N and BSi measurements, the calibration curves always produced $R^2 >$ 99.9% compared to the standard samples. This is regarded as good data quality.

The standard deviation (SD) is a measure of average variability in a data set. It is calculated from the mean value and if the SD is a large number (relative to the size of the mean value) there is a large spread of the data. Individual data points might then be far away from the mean value. The mean ± 1SD covers 68.27% of the data values in the set (given a normal distribution of the scores). Multiplying the SD with 1.96 calculates 2SD. 95.44% of the data points in the set lie within the mean ± 2SD (Wheater & Cook 2000; Salkind 2008). The SD is widely used for radiocarbon dates but here it has been applied for TC and N analysis as well.

The standard error of estimate (SE) tells about the accuracy of a prediction and may be calculated either from the SD or the regression line. The SE indicates how much on average the data differs from the prediction, and it tells about the accuracy of the data. A better correlation gives a lower SE. If the standard error is zero, there is no difference at all between our estimate and the actual data points (Wheater & Cook 2000; Salkind 2008).

For N analysis the mean value of measured

standards was 10.40%, which differs by 0.39% from the projected value (10.36%). 10.40 ± 0.19 accounts for 2SD (covering 95% of the data) and SE is 0.02. For TC analysis the mean was 70.89 which differs by 0.28% from the projected value (71.09). 2SD is 70.89 ± 0.97 and SE = 0.12.

3 Results and interpretation

3.1 Core examination, microscopic inspection and macrofossil analysis

A lithological log of the deposits is shown in Figure 8 and a complete description of every unit is presented in Appendix 1. Differences between the overlapping cores occur in some places, also noted in Appendix 1. Here follows a general description of the deposits.

The cores are all very dark in colour, compact and mostly very fine-textured, and it was therefore difficult to distinguish and separate between the different units. Rather than clearly different lithologies, the deposits are very similar but with a varying degree of decomposion. The dominating lithologies are humified fen peat and gyttja-like fen peat. Units and horizons of minerogenic-rich sediment and several clasts of silt also occur. Subsampling and microscopic analyses improved the lithological descriptions.

The humified fen peat is dark- to very dark brown and well decomposed, but coarse organic matter is abundant in many units. The lowermost unit is a highly humified fen peat which is extremely well decomposed and almost completely lacks macrofossil fragments. The gyttja-like fen peat is dark brown to very dark brown and contains small but various amounts of coarse organic matter. Due to the laboratory results, previous studies and knowledge about the site, the gyttja-like fen peat and the highly humified fen peat are interpreted as extremely decomposed peat units, although they are partly very gyttja-like. The deposits might have been subject to both subaerial decomposion and reworking (e.g. if the organic particles are transported and temporarily deposited in the surroundings several times before the final deposition in the wetland). In several of the units increased minerogenic matter results in lighter colours. Silty laminations are common in the middle and upper parts of the sequence.

The minerogenic-rich units are dark-coloured, thin (maximum a few centimeters), and sometimes with a tilted geometry. Some of them are possibly discordances. They consist of light-coloured and glassy minerals; mostly feldspars and glass or tephra particles, dark minerals; often biotite, perhaps also minor amounts of pyroxene or amphibole. Pumice, small pebbles of trachyte and grains of a reddish, unidentified mineral are present to a minor extent. At lower concentrations, the minerals found in the minerogenic-rich units are also seen in the organic-rich units. Organic material in the minerogenic-rich units reflects the material of the units above and below. A possible explanation of the minerogenic-rich units may be that certain erosion events such as thunder storms with heavy rain increased surface run-off around the basin. No pure tephra layers have been recognized, and it is more likely that tephra particles are spread out and incorporated into all the units.

Beige to grey coloured clasts of silt are present in all cores, ranging from a millimeter to a few centimeters in size. They always have sharp boundaries to the surrounding deposits and contain almost entirely light-coloured minerals. Since they are more abundant in or close to minerogenic-rich units they may as well be erosion features.

Results from microscope- and macrofossil analysis are presented in Table 2. In general the bottom units (unit 1-7, see Figure 8 and Appendix 1) contain very few macro remains apart from fern sporangia and some insect remains, which are very common throughout the sequence. Unit 6 contains a higher amount of plant macrofossil material and much of it originates from grasses and higher plants. This may be interpreted as an outwash event or a local vegetation change. Units 8-10 are dominated by dark coloured wood fragments. Seeds of the small herb *Callitriche christensenii* start to occur in unit 9 and are very common through the upper part of the sequence. Units 12-15 are a continuation of that, but with a higher and variable content of light-coloured, floating remains of grasses or higher plants. Unit 11 differs from the units below and above since it contains much more remains of higher plants, resembling the samples in the upper part of the stratigraphy. Even for unit 11, a short-lasting local change in vegetation or an outwash event is a possible explanation of the variation. Units 16-19 are rather variable in content and contain wood fragments, minerogenic sediment and remains of higher plants. Units 20-26 are all characterized by light-coloured plant remains (even though unit 24 contains some more dark coloured wood fragments).

3.2 Radiocarbon dating and age-depth model

The radiocarbon dates are presented in Table 3 and the age-depth model is shown in Figure 8. Most dates seem to be accurate, but two dates in the lowermost core, at 591.0 and 642.5 cm and one date in the uppermost part, at 211.0 cm, display diverging ages. They are interpreted as too old and are not included in the model (although shown in the graph). Reworking of the deposits is a likely explanation of too old ages, especially with respect to the environmental interpretation of the site. Another explanation could be a hiatus, but this idea is rejected due to the visible inspection of the deposits and the proxy-data record. Neither of them show any sign of a hiatus. The uppermost sample (211.0 cm) could perhaps be appropriate and it would then indicate large accumulation differences in the top of the sequence.

The agreement between the age model and the radiocarbon dates (the overall agreement index) is

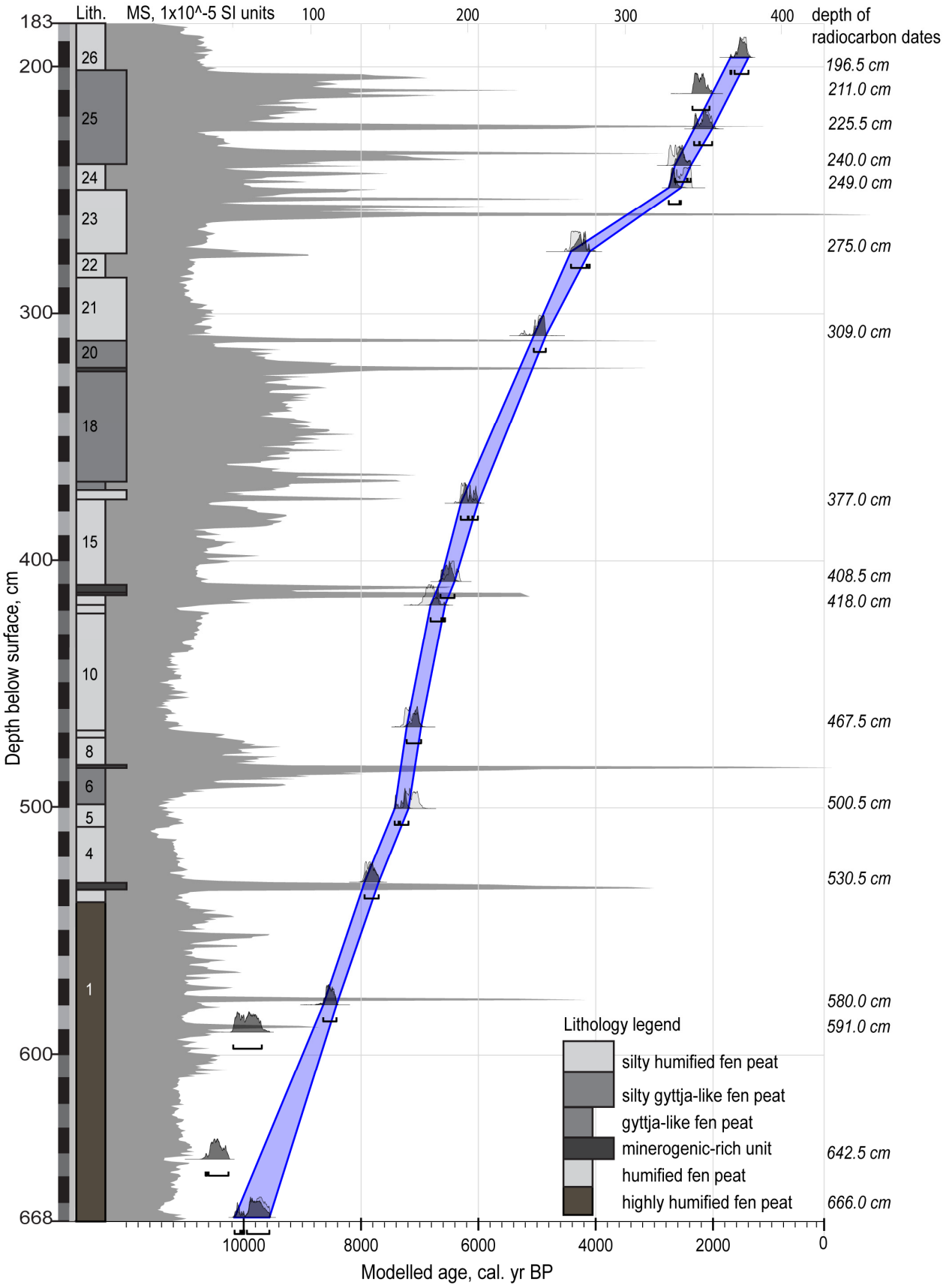

Fig. 8. The lithological log, the age model and MS results. 2SD are used for the age model and it is also shown for each calibration of dates. MS results are here limited to a maximum value of $450*10^{-5}$ SI units although the highest peaks reach about $1000*10^{-5}$ SI units.

Table 2. Results from microscopic and macrofossil analysis.

U.	Findings
1	Small glass/tephra particles, insect remain, fern sporangium. Very little material at all.
2	Insect remains. Almost nothing left after sieving.
3	Abundant in biotite and glass/tephra, some pumice. Fine-grained minerogenic clasts. Many fern sporangia, cf. *Acaena* seed, insect remains, insect eggs?* Some large and small unidentified plant material. Minerogenic-rich unit, LOI = 23%.
4	Abundant in insect remains, wood fragments, leaf**, cf. *Poaceae* seed.
5	*Rostkovia tristanensis* seed*,* glass/tephra particles, fern sporangia, some grass fragments (light-coloured, floating, elongated pieces).
6	Abundant in fern sporangia, some wood pieces, many fragments of grasses and higher plants including roots and epidermis. Some fine-grained minerogenic matter (biotite and glass/tephra), insect remains. Insect eggs*
7	Rich in minerogenic material: glass/tephra, trachyte, biotite and another dark mineral. Fine-grained minerogenic clasts. Insect remains, piece of wood, insect eggs?*, cf. *Ranunculus* seed, fern sporangia, higher plant remains. Minerogenic-rich unit, LOI = 8%.
8	Seeds of *Poaceae* sp., *Chenopodium* cf. *ambrosioides, Ranunculus carolii,* and *Cyperaceae* (e.g. *Carex*) or *Polygonaceae*. Many fragments of roots or wood, dark-coloured and not floating. Glass/tephra particles.
9	*Callitriche christensenii* seeds, insect remains. Fragments of roots or wood, dark-coloured.
10	*Callitriche christensenii* seeds*,* wood fragments (dark-coloured) and some grasses, biotite, some glass/ tephra.
11	Many *Callitriche christensenii* seeds. Insect remains, some glass/tephra, less wood fragments than below, more fragments from grasses and higher plants (as those in the upper samples). Well disintegrated sediment.
12	Abundant in wood fragments and grasses. Insect remains, seeds of *Callitriche christensenii,* glass/tephra, biotite.
13	Glass/tephra, also biotite, another dark mineral and trachyte/pumice. Pebbles of trachyte (cm size). Beetle wing, many fern sporangia, pieces of wood, unidentified plant remains, seeds of *Acaena* sp., *Poaceae* sp. and *Callitriche christensenii*. Minerogenic-rich unit, LOI = 11%.
14	Minerogenic material; mostly glass/tephra, also biotite, trachyte and red mineral. The mineral grains have a small grain size. Many fern sporangia, insect remain, beetle wing, seed of *Poaceae* sp., seed-shaped particle***, catkin scale or fruit (from unknown plant), some light-coloured plant remains, occasional wood pieces. Minerogenic-rich unit, LOI = 15-24%.
15	*Callitriche christensenii* seeds, insect remains, sparse wood fragments and grass remains.
16	Abundant wood fragments, *Callitriche christensenii* seeds, *Poaceae* sp. seed, insect remains.
17	Insect remains, some very fine-grained minerogenic material (light and dark coloured), some small peat remains, many fern sporangia. Moss leaf of *Kiaeria* cf. *pumila*. In general not so much macrofossil material left after sieving.
18	*Callitriche christensenii* (plenty of seeds), many small, unidentified plant remains, epidermis, lots of fern sporangia, insect remains, seed of *Poaceae*, leaf**, moss leafs of *Kiaeria* cf. *pumila* and *Bryum* sp., some small wood fragments, insect egg?* Sparse minerogenic contents of glass/tephra, some pumice/trachyte and biotite.
19	Minerogenic material; mostly glass/tephra and biotite. Some trachyte and red mineral. Seed of *Rostkovia tristanensis,* seed-shaped particle***, insect remains, piece of wood, unidentified plant remains/grasses. Minerogenic-rich unit, LOI = 9%.
20	*Callitriche christensenii* seeds, *Juncus* cf. *rostkovia* sp. seed, several beetle wings, small insect remains, piece of big insect, fern sporangia, seed-shaped particle***, some grass remains.
21	Seeds of *Callitriche christensenii*, seed of *Juncaceae* sp.****, insect remains, insect eggs?*, some grass remains.
22	Grasses, insect remains, grass seed? Fern sporangia, glass/tephra, abundant small and light coloured fragments of grasses.
23	*Callitriche christensenii* seeds, insect remains, glass/tephra, insect eggs?* Small grass fragments.
24	*Callitriche christensenii* seeds, many glass/tephra grains, insect remains, insect eggs?* Small grass fragments and dark wood pieces, seed of *Juncaceae* sp.****
25	*Rostkovia* sp. seed, fern sporangia, insect remains and grass remains.
26	*Callitriche christensenii* seeds*,* insect remains, insect eggs?*, grass remains.

Small, very round particles, black or bright, possibly insect eggs

**Spiky leafs of the same kind as found in the bottom of 1st Pond (37.000 cal. BP). Unidentified species.

***Unknown seed-shaped particle, size similar to seeds of *Callitriche christensenii*.

****A small seed of *Juncaceae*, of a species not mentioned in the field guide by Ryan (2007).

Table 3. Radiocarbon dates from the analysed cores. Bulk samples of peat was used for all samples.

Depth (cm)	^{14}C age BP	Cal. yr BP (SH04)	Lab no.
196.5 ± 0.5	1650 ± 50	1489 ± 120	LuS 9155
211.0 ± 0.5	2240 ± 50	2193 ± 143	LuS 9468
225.5 ± 0.5	2190 ± 50	2151 ± 160	LuS 9467
240.0 ± 0.5	2580 ± 50	2559 ± 193	LuS 9413
249.0 ± 0.5	2490 ± 50	2529 ± 178	LuS 9466
275.0 ± 0.5	3940 ± 50	4323 ± 174	LuS 9154
309.0 ± 0.5	4420 ± 50	5053 ± 218	LuS 9153
377.0 ± 0.5	5485 ± 55	6194 ± 190	LuS 9152
408.5 ± 0.5	5710 ± 55	6454 ± 149	LuS 9151
418.0 ± 0.5	6035 ± 55	6812 ± 143	LuS 9150
467.5 ± 0.5	6295 ± 55	7125 ± 149	LuS 9149
500.5 ± 0.5	6280 ± 55	7120 ± 146	LuS 9148
530.5 ± 0.5	7065 ± 60	7826 ± 128	LuS 9147
580.0 ± 0.5	7815 ± 55	8527 ± 115	LuS 9412
591.0 ± 0.5	8895 ± 60	9932 ± 244	LuS 9411
642.5 ± 0.5	9335 ± 60	10455 ± 196	LuS 9146
666.0 ± 0.5	8805 ± 55	9833 ± 286	LuS 9410

55.6%. Bronk Ramsey (2008) mentions 60% as the threshold for an acceptable agreement index, and this is close to that value. The average accumulation rate is 0.57 mm/year.

3.3 Magnetic susceptibility

The results of magnetic susceptibility are shown in Figures 8 and 9. The MS values are clearly linked to the minerogenic content of the deposits. Minerogenic-rich units and large clasts of silt give high-amplitude, short-lasting peaks. Silty deposits show up as an average rise of MS and larger fluctuations within the units than the more organic units. This is apparent in the upper parts of the sequence (e.g. around 350 cm depth) where more lithological changes, including silty laminations and silty-sandy horizons, occur. The most organic units show very low and stable susceptibilities but the very low values in the lowermost core are also affected by the smaller core diameter (5 cm compared to 7.5 cm).

3.4 Loss on ignition

The LOI results are presented in Figure 9. The sequence shows large changes with values spanning from 6 to 89%. The humified fen peat reaches the highest organic contents, over 80%, while the highly humified fen peat units and the gyttja-like fen peat have about 75% or lower.

The data display some general, long-lasting trends and some rapid changes with high amplitude. The latter changes are related to the minerogenic-rich units (e.g. at 534 cm) and the clasts of silt (e.g. at 578 cm), which both mainly consist of minerogenic matter. The general, long-lasting trends mirror the minerogenic content and silty laminations of the organic units. The two large-scale LOI decreases in the upper half of the sequence (at 390-310 cm and 280-210 cm) are most likely due to a higher content of sand and silt in general.

A comparison between LOI and TC results gives a slightly lower ratio than expected, on average LOI/TC = 1.7 (see data in Appendix 2). The result is very consistent except for a few outliers.

3.5 Carbon and nitrogen

The carbon and nitrogen curves follow each other closely throughout the core (Fig. 9). This is most obvious in the minerogenic-rich units where both TC and N decrease rapidly, but it is also valid for all major changes in the sequence, e.g. silty units show a clear lowering of the values of TC and N simultaneously. The humified fen peat sequences have the highest values of TC (45-50%) and N (2-3%) while the highly humified and reworked gyttja-like fen peat and the highly humified fen peat have lower values (TC 20-35%, N 0.7-1.5%). The C/N ratio varies between 17 and 32. The highly humified fen peat and the gyttja-like fen peat have a ratio around 27, and the humified fen peat around 23. The C/N ratios are in general high which indicates a dominance of terrestrial sources for the organic material. An additional measurement of recent peat from the surface of 1st Pond on Nightingale was performed. The result, C/N = 26, is close to the average peat values in 2nd Pond and this confirms the typical C/N ratio for the site. It points towards a sustained terrestrial environment (a wetland) throughout the Holocene, and it also strengthens the lithological interpretations.

3.6 Biogenic silica and diatom concentrations

Results from the BSi measurements are shown in Figure 9. The values are all very low in the lower part of the core and show a slightly increasing upward trend. Even though a few small peaks are visible, and the variations are larger in the upper half of the sequence, all the values are at the limit of detection for the method. The variations should therefore be interpreted with caution. It suggests that a very large extent of the BSi and DSi resources are recycled in the water, thus not being buried and recorded in the deposits (see e.g. discussion in Conley and Schelske (2001) for further details). The small amounts of silica available in the 2nd Pond wetland are most likely recycled to a very high extent.

The low BSi values also correspond well to the diatom record. In Table 4, BSi and diatom concentrations from four samples from the core sequence in the central part of the wetland and four samples from the

littoral core (this study) are presented. There is a strong relationship between BSi and diatom concentrations, and all the samples with the lowest BSi ratios completely lack diatoms, whereas those with slightly higher values contain diatoms. We may thus validate the BSi measurement and conclude that the BSi results are reliable although the values are very low. The diatoms in samples from both the central part of the wetland and the littoral core are few and poorly preserved. In the former cores, higher diatom concentrations occur concurrently with increased magnetic susceptibilities. This relationship has not been tested in the littoral stratigraphy, since diatom concentration was calculated only at four randomly picked levels. A similar relationship is likely, but additional diatom counts would be needed to confirm or reject the hypothesis. The low BSi and diatom concentrations are signs of a very nutrient-poor wetland and the diatom flora (mostly *Pinnularia* spp.) indicates an acid environment.

Table 4. Diatom concentrations and biogenic silica content from samples in the central part of the wetland and from the littoral core (the main core of this study). Diatom concentrations are calculated as total diatom valves/1 g dry sediment.

Core loc.	Depth, cm	BSi, wt%	Diatom conc.
Littoral	414.5	0.11	0
Central	713-715	0.18	0
Central	110-112	0.19	0
Littoral	410.8	0.27	0
Littoral	223.3	0.44	825 417
Central	231-233	0.59	4 930 530
Central	667-669	0.79	4 950 211
Littoral	208	1.33	2 928 265

3.7 Correlation test

The results of the correlation tests (Pearson's product moment correlation and the coefficient of determination, R^2) are shown in Table 5. As already noted, MS, LOI, TC and N have a clear covariance, in contrast to the BSi which shows a very low correlation to all of the above mentioned variables. However, and as expected, the BSi has a close relationship to the diatom abundance, but the relation between BSi and C/N is surprisingly good. It is a strong correlation but since the BSi values are all so low that they are close to the detection limit and the C/N ratio is slightly unpredictable, any interpretations of the covariance would be very speculative.

4 Discussion

4.1 Synthesis of core examination and laboratory results

2nd Pond has most likely remained a fen throughout the Holocene. From time to time the precipitation rate increased and higher fluxes of eroded material from the surroundings reached the wetland. Small areas of

Table 5. Correlation tests (Pearson's product moment correlation and the coefficient of determination, R^2) for MS, LOI, TC, N, C/N and BSi results.

Parameters	Pearson's	R^2	Variation in common
MS – BSi	0.067	0.004	0.4%
MS – LOI	-0.616	0.380	38.0%
MS – C	-0.625	0.390	39.0%
MS – N	-0.583	0.340	34.0%
MS – C/N	0.161	0.026	2.6%
BSi – LOI	-0.192	0.037	3.7%
BSi – C	-0.185	0.034	3.4%
BSi – N	-0.040	0.002	0.2%
BSi – C/N	-0.477	0.227	22.7%
LOI – C	0.966	0.933	93.3%
LOI – N	0.909	0.826	82.6%
LOI – C/N	-0.213	0.045	4.5%
C – N	0.948	0.898	89.8%
C – C/N	-0.245	0.060	6.0%
N – C/N	-0.508	0.258	25.8%
BSi – diatoms*	0.992	0.984	98.4%

*Values of diatoms from data presented in Table 4 (four measurements from the central part of 2nd Pond and four from the littoral core).

open water or more swampy areas may have occurred in the wetland, but even during these times the deposits have been completely dominated by terrestrial material and no major, continuous algal growth has occurred. Subaerial decomposition and reworking of deposits is a likely explanation for the extremely well decomposed lithologies. The highly decomposed units of gyttja-like fen peat occur associated with the events of higher humidity. These are also characterized by increased erosion displayed as higher MS and more commonly occurring silty clasts and minerogenic-rich units and horizons. These episodes are also clearly seen in the MS record.

The minor vegetation- and lithology changes (apart from the minerogenic-rich units) and the relatively small changes of C/N ratio within the organic deposits indicate that only limited changes of the water table, in relation to the vegetation level, took place. If larger changes would have occurred, this should be seen as different lithologies (pure gyttja during higher water table) and larger differences in both C/N ratio and macrofossil results. The highly humified fen peat and the gyttja-like fen peat have probably been exposed to subaerial decomposion since the water-atmosphere interface is a very dynamic environment. During the formation of those units the water table was probably slightly lower in relationship to the vegetation level. The precipitation-rich events were probably associated with a warmer climate, thus increasing the

evaporation and preventing a water table rise.

Vegetation changes in and around the wetland may have occurred, but without more detailed and quantitative macrofossil analysis or pollen analysis more detailed conclusions cannot be made. The changes found in the macrofossil record may be due to minor water table changes or increased erosion. It is likely that the ground-water flow in the basin is very low. This conclusion is based upon the very low nutrient levels of the site, since a large ground-water flow would bring nutrients from the bedrock to the pond.

It seems very likely that the events characterised by higher MS and lower OM are due to increased erosion explained by higher humidity and precipitation rates, and preferably connected to warmer temperatures according to the discussion above.

For the basis of the environmental interpretation, the lithostratigraphy has been divided into 13 sections (A to M, see below and Figure 9). Some of them are major events (sections B, F, J and L) with increased precipitation rates. D and H are interpreted as minor events which may have a more local or short-lasting origin. In between these events the deposits display stable and much less variable proxy parameters (sections A, C, E, G, I, K and M). During these periods the climate was possibly drier.

Section A, 668-563 cm

The lowermost section is a massive unit of highly humified fen peat characterized by low MS and high TC, N, C/N and LOI. All parameters are very stable throughout the unit. A likely explanation (due to the high LOI and C/N values and the highly disintegrated deposits), is that the deposit has been subject to subaerial decomposion and reworking (shown by e.g. too old radiocarbon dates). The large MS peaks and a correlating dip in other parameters are directly related to clasts of silt. The transition into section B is gradual.

Section B, 563-542 cm

Lower LOI, TC and N characterize the section. MS is slightly higher than below. This is a continuation of the lowermost section (A), but with slightly higher erosion rates which bring minerogenic matter from the surroundings and decrease the content of organic matter. It is interpreted as a large-scale climate oscillation although the differences are somewhat subtle in the proxy records. The transition into section C is sharp.

Section C, 542-536 cm

Section C is a thin unit of peat characterized by high LOI and C, and low MS values. Proxy data are similar to section A but the organic matter content is even higher and the deposit has a slightly different texture with a higher water content. The transition towards section D is very rapid and a discordance is possible.

Section D, 536-530 cm

D is a short event, characterized by a minerogenic-rich sediment unit with high MS and C/N ratio, and low LOI, TC and N values. It is interpreted as a very short-lasting event and possibly only local, such as temporarily increased surface run-off during a single thunder storm with heavy rain. The abrupt start and end of the event favour such an explanation.

Section E, 530-494 cm

This is a continuation of C with similar proxy values. The transition into F is gradual.

Section F, 494-470 cm

A unit of gyttja-like fen peat occurs in the first part of section F. It is then followed by a minerogenic-rich unit and laminated silty peat. MS increases throughout, but especially in the minerogenic-rich unit. LOI, TC and N clearly decrease throughout the unit while C/N is high. The deposition rate is high. A change in vegetation is inferred above the minerogenic-rich unit, seen as abundant wood fragments in macrofossil analysis samples. The wetland species *Callitriche christensenii* first appears in this section and it clearly indicates a wet environment.

Section G, 470-422 cm

In the proxy data record section G is very similar to E and C, suggesting the same depositional environment and climate, even though the vegetation resembles the newly established flora record with wood fragments, but also a varying content of higher plants and grasses.

Section H, 422-410 cm

Section H is represented by a minerogenic-rich unit, with high MS and C/N ratio and low LOI, C and N. It is probably a local event similar to D, a conclusion drawn from the marked rise and fall of proxy values, and the fast re-establishment of proxy values similar to those in section G afterwards.

Section I, 410-391 cm

Humified fen peat accumulation occurs again and the section is similar to G but with slightly increasing MS upwards towards section J.

Section J, 391-309 cm

This is a large-scale and long-lasting event with increased MS and C/N ratio, and decreased LOI and TC values. First more minerogenic material and silty laminations in the deposit are noted. Then a change in vegetation occurs, now dominated by grasses and higher plants. Several rapid oscillations and minerogenic-rich units and horizons are preserved in the lithology. A change into gyttja-like fen peat occurs and the middle part of section J is rather stable. In the upper part some rapid oscillations (including a minerogenic-rich unit) occur again. Some of the subunits with minerogenic-rich sediment may be erosive, although no major signs

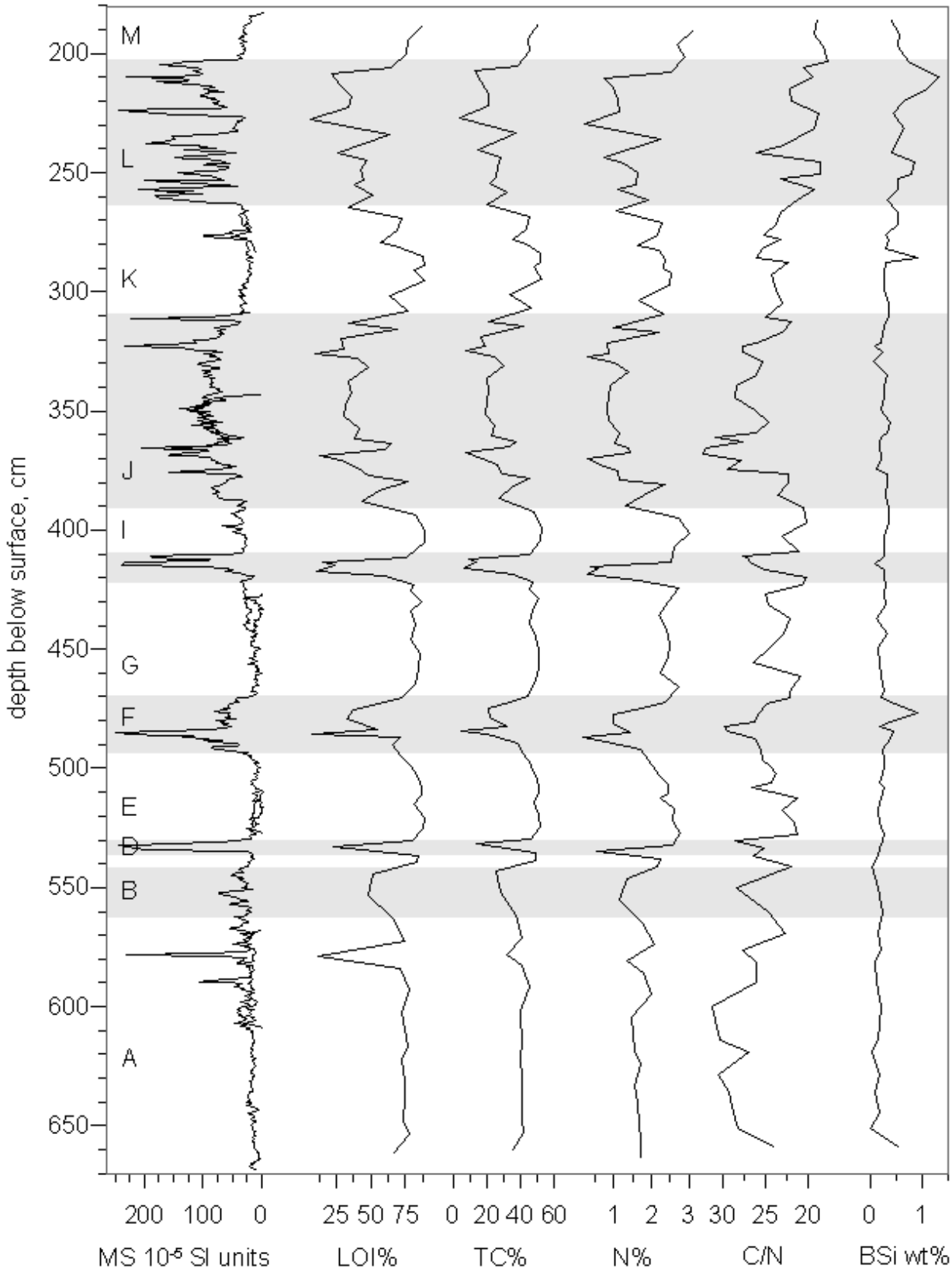

Fig. 9. MS, LOI, TC, TN C/N and BSi-data plotted against the depth (vertical axis). The events interpreted as periods of extensive erosion due to higher precipitation rates are shaded in the graph and each section is named (A-M). MS results are here limited to a maximum value of $250*10^{-5}$ SI units although the highest peaks reach about $1000*10^{-5}$ SI units.

are seen in the chronology. A sign of the increased erosion is the occurrence of leaves of *Kiaeria* cf. *pumila*, which is a moss species living in dry environments, on stony soils and rocks (Ochyra 1998). These

must then have been transported by erosion to the wetland. The transition into K is gradual.

Section K, 309-264 cm

Humified fen peat accumulates in K which is similar to the previous stable periods (such as A, E and G) between the precipitation-rich climatic events. Higher plants and grasses dominate the preserved deposit. The transition into section L is sharp.

Section L, 264-203 cm

Fen peat formation first continues, thereafter gyttja-like fen peat forms. MS is high and very variable throughout and associated with decreased OM (LOI and TC). N and C/N ratio are low, but a very small increase of BSi values is visible. In the middle of the section, a short period of inversed data values (lower MS and higher OM) is present. It ends abruptly at a minerogenic-rich subunit, which might be erosive at its base. Similarly to J, section L is a large-scale and long-lasting event. The transition into the uppermost part of the stratigraphy is very sharp.

Section M, 203-183 cm

Fen peat formation with low and stable MS values and very high OM and N occurs until the top of the core.

4.2 Comparison with a previous study

The doctoral thesis by Ljung (2007) and the paper by Ljung and Björck (2007) present results from the central part of 2nd Pond. An almost 10 m long sequence was dated with 53 ^{14}C datings on which the detailed chronology relies. The used proxy methods are core descriptions, MS measurements, TC-, N- and S- analysis and pollen analysis. Some main conclusions of the climate development of Nightingale Island are as follows:

1. A transition from peat to gyttja deposition at 8600 cal. BP represents the establishment of the modern ocean-atmosphere circulation in the Southern Hemisphere. SHW moved northwards bringing more precipitation and a colder climate to the area. This also coincides with the end of the Antarctic climate optimum.
2. Between 8600 and 500 cal. BP gyttja is deposited. The lake is overgrown around 500 cal. BP when peat again starts to accumulate.
3. During the sequence, short recurrent oscillations (100-1000 years), thought to represent periods with higher precipitation, are recorded. They are recognized in the proxy data as increases of MS and C/N ratio, decrease of C and N and a specific pollen assemblage containing more pollen from distal parts of the catchment area. The higher precipitation probably depends on short, warm events when SST increased or increased intensity of the SHW. However, no increased sulphur content (due to sea spray) was found associated with the erosion events, which would be expected if the erosion was due to increased wind activity. Since the Atlantic Meridional Overturning Circulation (AMOC) acts as a control for the SST around Tristan, periods of weaker AMOC are associated with increased SST. These periods are to some extent also found in the North Atlantic as events of increased IRD. Thus an interglacial bipolar see-saw could be in action.
4. The 8.2 ka cold event which is well recorded in the NH is suggested to be present in the sequence as one of the short precipitation-rich oscillations. This points towards a bipolar see-saw that can be active even in interglacial times.

The results of the study in this thesis are well comparable to those by Ljung and Björck (2007) and the proxy record displays similar results, both in terms of absolute values and in the characteristic pattern. It should however be noted that even during examination and logging of the core from the central basin, the lithologies were hard to classify and the units interpreted as gyttja corresponds to the gyttja-like fen peat in the littoral core (K. Ljung personal communication 2011). Figure 10 shows a comparison of data where events thought to represent more precipitation-rich periods during the Holocene are clearly seen. The central pond core usually displays the most severe erosion events, while the littoral core is more sensitive to changes, both local and larger-scale ones. The two cores also help to distinguish between the very local phenomena and the larger changes, which influence the whole pond and possibly much larger regions than that as well. The exact timing of the precipitation-rich events sometimes differs between the sites. This may be explained by differences between the sites and the chronologies. Some radiocarbon dates do not fit to the chronologies and the littoral core is more sparsely dated. The uncertainties of some dates are rather large which again makes the exact timing hard to determine and verify.

Below follows a comparison of each event which is thought to represent precipitation-rich oscillations in this study and in the study by Ljung and Björck (2007) (Fig. 10).

Around 9500 cal. BP

A peak of *Phylica arborea* trees, herbs and grasses is seen in the pollen record in the study by Ljung and Björck (2007), but these changes are not reflected in the MS, TC and C/N records. Nothing is seen in the results from the littoral core, which might be due to the very homogenized and decomposed deposit or other differences between the sites. Perhaps this event is more local or temporary than previously though.

9000-8000 cal. BP

Between 9000 and 8000 cal. BP a general transition

occurs both in the littoral and central part. MS increases slightly and other proxies become more variable. C/N decreases in both records, and the site probably gets wetter and swampier. The largest change occurs at 8600 cal. BP. The peat-to-gyttja transition at 8600 cal. BP in the central core is thought to represent the establishment of modern-day global circulation which brought more precipitation to the Tristan da Cunha archipelago (Ljung and Björck 2007). No counterpart to this change is found in the littoral core; neither in the lithological logg nor in the proxy data record, apart from a decreasing TC trend and more variable MS. The deposits close to the shore might have been subject to secondary processes or very extensive decomposition, destroying any clear signal. Reworking can also explain the apparently too old radiocarbon ages in the lowermost unit. Independently of the explanation, a confirmation of an establishment of modern-day large-scale circulation around 8600 cal. BP is not clear, but the littoral core does not contradict such a change. The start of more variable proxies 9000-8000 cal. BP is probably the only such sign in the littoral core. The appearance of *Callitriche christensenii* around that time in the record by Ljung and Björck (2007) is a clear indicator of the onset of precipitation-rich conditions. The species enters slightly later in the littoral core, but this may be due to the rather coarse and unquantified macrofossil analysis of the littoral core.

Around 8500 cal. BP

A small dip in TC and N and a peak of MS is found, also corresponding to more tree and grass pollen. In the littoral core, this is seen as slightly increased MS and a clast of silt. Although not the primarily expected response, it might verify the signal from the central core.

8300-8000 cal. BP (section B)

A clear oscillation is seen in the record by Ljung and Björck (2007). A change is also seen in the littoral core, and it corresponds to section B (see previous synthesis). This might represent a SH response to the 8.2 ka cold event in NH. If the higher precipitation was caused by increased SSTs (Ljung *et al.* 2008) this strengthens the hypothesis of a bipolar seesaw during the Holocene even further.

7900-7800 cal. BP

The short peaks of section D in the littoral core are not seen in the other core, and the hypothesis that it is a very local phenomenon is verified. Since no major problems with radiocarbon dates and the chronologies are displayed within this section, it is also considered unlikely to be part of the 8.2 ka event.

7300-7100 cal. BP (or alternatively 7500-7300 cal. BP, section F)

The events shown in the different cores are not perfectly matched in time, but this is probably explained by the different age models. Some of the radiocarbon dates in the study by Ljung and Björck (2007) do not fit to the model, and problems with the chronologies are suggested to be responsible for the imperfect synchrony.

6750-6550 cal. BP (section H)

Section H was interpreted as a very local change in the synthesis of the littoral core, but since it has a very good counterpart in the record from the central part of the wetland as well, it is probably a more widespread event. The temporal synchrony between the cores is almost perfect, and definitely within the uncertainties. The OM content is substantially lowered in both records. This event also highlights that the climate changes and their responses in the proxy record can be remarkably fast, especially if they represent large-scale (hemispheric) changes.

6300-5000 cal. BP (or alternatively 6400-5400 cal. BP, section J)

The onset at 6400-6300 seems to be well synchronised and the pattern is very similar with large fluctuations in the beginning and then slightly more stable proxies. However, the ending of the event is about 400 years earlier in the central pond core (at 5400 cal. BP). This could perhaps be due to the higher sensitivity expected close to the shore, but it could also be due to the chronologies. In the age model by Ljung and Björck (2007), some radiocarbon dates have been rejected around that depth. At the same time, the uncertainties of the ages in the littoral core are rather large and the dates are not closely spaced. Since the pattern of the oscillation is very similar in both cores, and no major lag between the sites has been found elsewhere, it is most likely that it is the same event and lasting for the same time, but displayed differently. It is most likely due to dating uncertainties in either or both of the cores.

Around 4500 cal. BP

The peak found in the study by Ljung and Björck (2007) has no obvious corresponding peak in the littoral core. The small peak found at 4300 cal. BP could perhaps be the littoral response, but it is much smaller. Due to the dating uncertainty just below it, this is not an unlikely solution, but no certain conclusions may be drawn in this case.

3700-1700 cal. BP (section L)

In this interval, proxy data from the littoral core show a longer period of sustained increased surface runoff/erosion between 3700 and 1700, possibly with a break between 2350-2200 cal. BP. The record from the central part of the wetland shows two shorter oscillations lasting between 3050-2800 and 2650-1700 cal. BP. The differences in occurrence are most likely due to the different positions. It is likely that during short,

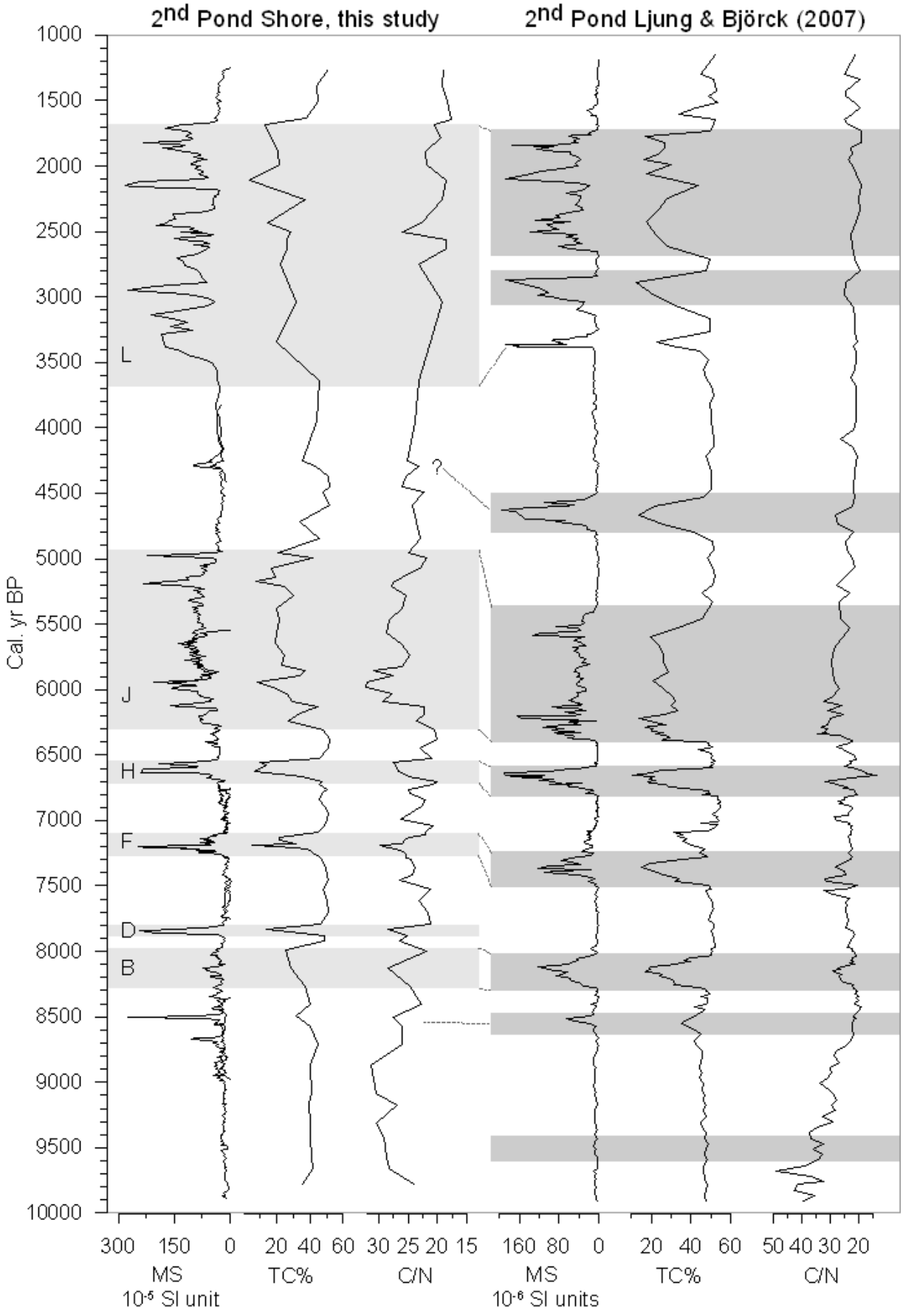

Fig. 10. A comparison between MS, TC and C/N ratio from this study (left) and the study by Ljung and Björck 2007 (right). The erosion- and precipitation rich events discovered in each study are marked.

calmer intervals, the erosion signal did not reach all the way to the central site. The opposite is also possible: if the littoral core is disturbed by more local processes or reworking, the central core might better reflect large-scale climate changes. In this case, erosion might have been lower several times during the oscillation, as shown in the record by Ljung and Björck (2007). There is also a question about the start of the oscillation or oscillations. In the littoral core the oscillation starts around 3700 cal. BP. In the central-basin core, a minor peak is seen in TC and MS at 3400 cal. BP, but it is not associated with a change in the pollen spectrum. Perhaps this minor change should anyway be interpreted as the start of the event in the central core. The timing is then better, although not perfect. Even here the differences might be due to the chronologies, since both the littoral core and the central core have some dates that do not really fit to the age models.

Summary

Due to the above described comparison of data from the littoral core analysed in this study and the core from the central part of the 2nd Pond investigated by Ljung and Björck (2007) the following climate and environmental development at Nightingale Island is suggested. In the beginning of the Holocene warm and stable climate conditions occurred. SHW were probably displaced southwards (Ljung and Björck 2007). Between 9000 and 8000 cal. ago, SHW moved northwards and the average climate became colder and more humid (Ljung and Björck 2007). Several short oscillations of higher precipitation and erosion occurred. The first one of these took place around 8500 cal. BP. Between 8300-8000 cal. BP a larger oscillation took place, which coincides with the 8.2 ka event which is well known in the NH (see e.g. Thomas *et al.* 2007). Between 7300-7100 cal. BP the next oscillation occurred although the timing is a bit unclear (an alternative timing would be 7500-7300 cal. BP). From 6750 to 6550 cal. BP another precipitation-rich event took place, this time with a clear and well-matched synchrony between the investigated sites. Until this time, the oscillations were short-lasting, maximum 300 years. At 6400-6300 cal. BP a more long-lasting oscillation starts, but it is unclear if it lasted until 5400 or 5000 cal. BP, which is due to dating difficulties. Somewhere around 4500 cal. BP a short oscillation might have occurred, but the proxy records differ and no clear conclusion can be made. The last oscillation or oscillations occurred between 3700 and 1700 cal. BP. The start of the interval is unclear and the two sites differ from each other, but the changes during the oscillation were large and variable. A short period with lower erosion occurs 2350-2200 cal. BP, but the timing is unclear even in this case. The oscillation ends rapidly and synchronized at 1700 cal. BP and it is followed by stable climate conditions with lower erosion rates.

4.3 Alternative interpretations

Ljung and Björck (2007) interpret the changes in pollen assemblage during the oscillations as increased inwash of pollen from the distal part of the catchment. Their primary explanation of the humid oscillations are increased SSTs in the South Atlantic Ocean but there are also other possible interpretations of the data. Here follows a discussion on alternative interpretations of data and climate development.

One alternative explanation of the pollen record would be that an actual change occurred in the vegetation on the island. If climate became drier, the species living on higher, drier ground would expand their habitats, reducing the more moist-demanding species. This could also result in the changes found in the pollen record by Ljung and Björck (2007). The increased minerogenic content during the oscillations could then perhaps be explained by the drier ground which would make it more sensitive to the wind and thus enable more intense erosion.

Ljung and Björck (2007) preferentially coupled the environmental changes to large-scale climatic features such as SHW position and the strength of the AMOC. It is likely that some or all of the oscillations are due to such large-scale climate features, but other interpretations are also possible. Since the island is formed by volcanic activity, which has proved to be still active at least to some extent (Reagan *et al.* 2008), earthquakes are not unlikely in the area and these have the potential of opening new erosion surfaces which would lead to increased deposition of minerogenic material. Newly exposed rock- and sediment faces without vegetation would be a possibility for establishment of new vegetation with a different composition. Recurring earthquakes could perhaps explain the proxy changes, and the different lengths of the erosion events would then represent the magnitude or impact of the earthquakes. But if earthquakes are that common, there should be more signs of them in the environment. This is a strong argument against the earthquake hypothesis, but geomorphological and geophysical measurements would be one way of testing it.

Another plausible hypothesis is that the environmental changes are mostly related to wind intensity decoupled from precipitation. Since Nightingale Island is located in a very windy area, it is not unlikely that even stronger winds would bring loose material into the depression of 2nd Pond. If wind intensity increases, it would imply that SHW moved northwards. In South America a strong relationship between wind intensity and precipitation exists. Even though Nightingale Island has a much lower altitude compared to the Andes in South America, precipitation rates would increase at least to some extent if SHW moved northwards. Ljung and Björck (2007) used sulphur as a proxy for wind intensity, since higher wind intensities can be assumed to bring more sulphur-rich sea-spray. Although they concluded from the sulphur record that wind intensity was not notably higher during the erosion-rich events, sulphur is a somewhat problematic proxy to use. Other

ways of evaluating wind intensity would be needed to test the hypothesis.

The effective humidity may be increased by less evaporation, which would in turn be possible in a colder climate. Identification and counting of temperature sensitive algae, insects or other species would be one way of testing this hypothesis.

4.4 Literature study – causes of climate variations in the Southern Hemisphere

Many recently published studies deal with the SH climate development during the Holocene. Widespread signs of variable climate conditions are found, but the pattern is not consistent and the records rarely fit well between different sites. Variations in sea ice conditions around Antarctica, the strength of the subtropical high-pressure systems, latitude- or intensity changes of the SHW and oceanographic changes are among the discussed explanations for climate variability in the SH since the last glacial termination. Here a brief literature review presents some of the main suggestions for climate changes in South America during Holocene. The same processes might influence the climate on Nightingale Island.

At mid latitudes, the SHW may be the strongest controlling factor of the climate. One explanation of the varying records of SHW is that studies done at different latitudes will display a change of SHW differently with respect to humidity and precipitation (Waldmann *et al.* 2010). The site location in relation to topographic features such as the Andes also plays a major role since areas east of the Andes will be in a rain shadow of precipitation from the west (Mayr *et al.* 2007).

The relationship between the APF (Antarctic Polar Front), the ACC and the SHW are also discussed. Today strong SHW at the latitude of ACC prompt the oceanic circulation with deep-water formation and upwelling which is essential for the ocean circulation. If the SHW are shifted northwards or weakened, this may decrease the ocean circulation in the Southern Ocean as well as decreasing the CO_2 release from the upwelling CO_2-rich deep-waters (Moreno *et al.* 2010; Hodgson & Sime 2010). The sea-ice extent and the SST gradient in the ocean at different latitudes are also thought to be strong forcings of the position of the SHW (Bentley *et al.* 2009; Hudson & Hewitson 2001)

The establishment of ENSO/El Niño circulation, which strongly effects the humidity and upwelling of nutrient-rich deep-waters along the west coast of South America (Hess 2011), is suggested as responsible for climate change during the late Holocene (Jenny *et al.* 2003; Lamy *et al.* 2001). The long-term climatic impact of ENSO circulation needs to be further studied.

A relationship between solar insolation and climate change (summer SST) at high latitudes in the Atlantic sector of the Southern Ocean is evaluated by Nielsen *et al.* (2004). They conclude that changes show a correspondence to NH summer insolation during the early Holocene and to SH insolation during the mid and late Holocene. The investigated site is very close to the APF and a strong influence by the Antarctic climate is suggested for the unexpected change. On the other hand, Lamy *et al.* (2010) do not favour orbital insolation changes as an explanation for their recorded climate changes.

The spatial variations of the SHW are also a matter of debate: Among others, Waldmann *et al.* (2010) suggest that northward or southward migration of the SHW are responsible for climate fluctuations whereas Lamy *et al.* (2010) present a pattern where the core of the SHW are sometimes narrowed and strengthened and sometimes widened (preferably northwards) but weakened.

An interesting question is also: What type of processes lead to increased precipitation? This could be either when SHW are intensified in an area or when warmer ocean SSTs enhance evaporation and precipitation in an area, e.g. due to a southward shift of the westerlies (Ljung 2007; Ryan 2007). Today a strong relationship exists between the intensity of SHW and the precipitation along the western South American coast (Lamy *et al.* 2001), but SSTs are also known to be important for precipitation rates (Ljung 2007). When comparing the Tristan da Cunha archipelago with mainland records from South America it is important to be aware of the differences between the sites. It is possible that an intensification of SHW could result in increased precipitation, but since the location and the oceanographic positions of the sites are so different (islands in the middle of the ocean compared to a large land mass with a high mountain range) a straight-forward comparison may be difficult.

Two studies that may be comparable with the Tristan record are Lamy *et al.* (2001) and Jenny *et al.* (2003). The first study presents a record from the Chilean coast at 41°S. They find a long-term precipitation record with drier conditions 7700 to 4000 cal. BP and more humid conditions from 4000 cal. BP until the present. Superimposed on the long-term trend they find humidity variations with cycles of 900 and 1500 years, which are interpreted as shifts of SHW. These shifts might be forced by or related to Hadley cell intensity (atmospheric circulation at low latitudes) and ENSO circulation. Compared to the study presented in this thesis, the results by Lamy *et al.* (2001) both differ and show similarities: In terms of the general trends the record differs, but the pattern of shorter, cyclic oscillations corresponds well to our record. Especially a 900-year cycle seems to be well comparable with the shorter oscillations displayed in 2nd Pond.

The other study (Jenny *et al.* 2003) presents a water balance model for a lake in central Chile (34°S). They conclude that precipitation rates were very low in the beginning of the Holocene and until 8000 cal. BP. Between 8000 and 6000 cal. BP precipitation rate

increased, followed by another, more drastic, precipitation rise. Since 3000 cal. BP the lake level and humid conditions with high precipitation rates have been maintained. The dry conditions in the early Holocene are explained by a southward deflection of the SHW due to the strong subtropical high-pressure cell, while the late Holocene more humid conditions is explained by intensified SHW and perhaps also ENSO circulation. This humidity record fits well to 2nd Pond in some aspects: The early Holocene is dry, and then the precipitation increased, even though that started somewhat earlier than 8000 cal. BP in 2nd Pond, which could be explained by the latitudinal differences between the sites. A larger precipitation increase after 6000 cal. BP corresponds to the precipitation-rich interval that starts at 6300 cal. BP. After that, the records do not fit as well, since the period 5000-3700 cal. BP was drier at Nightingale. Moreover, after the precipitation-rich oscillation that lasted 1700 cal. BP, the Nightingale record displays drier conditions which do not correspond to Jenny *et al.* (2003).

Altogether, there is a lot of data around but they are hard to interpret and compare. It is obvious that the climate dynamics and the lead-lag factors are not understood well enough. Solar insolation, Hadley cells and the subtropical high-pressure systems as well as ocean circulation, SST gradients, sea ice extent and the ENSO development may influence SHW and SH climate at different time-scales and during different conditions. It is obvious that deeper knowledge of these dynamics is needed to reach an increased understanding of climate change in the SH.

5 Summary

5.1 Conclusions

The site 2nd Pond on Nightingale Island in the South Atlantic Ocean has been investigated. It is a nutrient-poor overgrown wetland. An almost five meter long peat sequence covers most of the Holocene (ca. 10000-1000 cal. BP) and it mainly consists of well decomposed fen peat. The proxy records (core descriptions, macrofossil analysis, MS, TC, N, LOI and BSi) reveal an interesting pattern of changes between precipitation-rich events and drier climate and environmental conditions in between the events. Here follows the main conclusions.

- During periods of normal (low) precipitation rates the proxy records are signified by a very high organic content and in general low MS. A well decomposed fen peat is being deposited most of the time. The deposit has a very terrestrial signal and it is almost exclusively made up by terrestrial plants and mosses growing on the surface. This is also confirmed by the absence of diatoms at many levels.
- The precipitation-rich events are characterized by decreased LOI, TC and N ratios and increased MS. Lithological changes associated with the events are mainly displayed as an increased degree of decomposion (possibly subaerial) and a higher minerogenic content of the deposit.
- The littoral core is a sensitive recorder of environmental changes and this is displayed in the proxy- and lithological records. To differentiate between very local changes and large-scale changes was sometimes difficult, but a better understanding was obtained by comparing this study with the results by Ljung and Björck (2007).
- A very similar pattern of the proxies are found when the results from the littoral site are compared to those of the central site of 2nd Pond (Ljung and Björck 2007). The differences are usually easily explained by the different locations of the cores (close to the shore and in the central part of the pond, respectively) and by dating uncertainties. This strengthens the hypothesis that short precipitation-rich events occurred during the Holocene. The study by Ljung and Björck (2007) also includes pollen analysis, and the pollen assemblages strongly support the interpretations.
- In the study by Ljung and Björck (2007) a major lithological shift is found around 8600 cal. BP and this has been interpreted as a northward shift of the westerlies. There is not any well marked change in the littoral core presented in this study, but some subtle signs of change are found. Due to the data presented in this study, there is no strong argument against the hypothesis, although it cannot be satisfactorily confirmed.
- Based on the comparison between this study and Ljung and Björck (2007) the following precipitation-rich events are suggested: around 8500, 8300-8000 (which corresponds to NH 8.2 ka cold event), 7300-7100 (or possibly 7500-7300), 6750-6550, 6300-5000 (or possibly 6400-5400) and 3700-1700 cal. BP. The precipitation-rich oscillations with increased erosion rates from the catchment area are represented by increased MS, decreased OM and a different pollen assemblage in the deposits (Ljung and Björck 2007).
- Studies from South America often show variation in terms of humidity and precipitation during the Holocene. The records differ much between different sites and there is yet no consensus about the changes. It is suggested that changes in the extent and intensity of the SHW have occurred but the precise mechanisms behind why, how and when they have varied are still to be revealed. SST and global ocean circulation seem to be important forcing factors and a bipolar seesaw pattern between the North and South Atlantic Ocean is possible, although it needs to be further studied.

5.2 Further implications

Through the analysis of 2nd Pond Shore peat sequence, increased understanding and verification of the results of Ljung and Björck (2007) is obtained. The assumption that the site has a large potential for climate reconstructions has been further established. Further studies of other sites in the Tristan da Cunha archipelago would possibly bring a higher level of certainty to the investigation and the conclusions about the timing of precipitation-rich events. It still cannot be excluded that some of the events which are here interpreted as large-scale climatic changes are much more local phenomena, e.g. only within the 2nd Pond wetland. This needs to be further studied. As shown by the short-lived oscillations, the climate system must be very sensitive since it has such a possibility to undergo very rapid changes. This is surprising when seen in the perspective of the slow global ocean circulation and there are probably many more discoveries to be made in the aim of better understanding the climate dynamics.

For further work on 2nd Pond, more radiocarbon dates or modelling of the ages would be one way to obtain an even more accurate match between the two studies of 2nd Pond. An extended and quantified macrofossil analysis would contribute with more information about the paleoenvironment, especially if a reference collection is available. Further studies of other sites are needed to better understand the magnitude of the precipitation-rich oscillations (e.g. Do they affect only Nightingale Island or the archipelago of Tristan da Cunha, or are they a large-scale feature that affects the whole SH?). What we have found so far could be signs of a large-scale, multi-centennial climate feature, and understanding its forcing mechanisms would greatly improve our knowledge about the dynamic climate system. It also brings the question about human environmental impact into the light. May we expect recurring precipitation-rich events at the mid latitudes in the SH even in the future, or has mankind's impact displaced or weakened these oscillations?

6 Acknowledgments

The technicians Åsa Wallin and Git Klintvik Ahlberg have both been helpful with the laboratory techniques, hints and tips, and nice company in the lab. Daniel Conley patiently and pedagogically helped out with the BSi analysis. The macrofossil analysis was performed in cooperation with Nathalie Van der Putten who showed an honest interest in the task. As assisting supervisors, Sofia Holmgren and Karl Ljung helped out in various situations, e.g. with discussing the results. Sofia Holmgren also performed the diatom counting and Karl Ljung was especially helpful with the age-depth model. My main supervisor Svante Björck is thanked for various help along the way and for his approach that he always has a few minutes for whatever questions I have. Finally, thanks for offering me the opportunity to work with the material from the fascinating Nightingale Island.

7 References

Baker, P. E., 1973: Islands of the South Atlantic. In: Nairn, A. E. M. & Stehli, F. G. (eds.): *The ocean basins and margins; Vol 1, The South Atlantic*, 493-553. Plenum Press, New York.

Battarbee, R. W., Jones, V. J., Flower, R. J., Cameron, N. G., Bennion, H., Carvalho, L. and Juggins, S. 2001. Diatoms. In: Smol, J. P., Birks, H. J. B. & Last, W. M. (eds.): *Tracking environmental change using lake sediments; Volume 3, Terrestrial, algal, and siliceous indicators*, 155-202. Kluwer Academic Publishers, Dordrecht.

Bentley, M. J., Hodgson, D. A., Smith, J. A., Cofaigh, C. Ó., Domack, E. W., Larter, R. D., Roberts, S. J., Brachfeld, S., Leventer, A., Hjort, C., Hillenbrand, C.-D. and Evans, J., 2009: Mechanisms of Holocene paleoenvironmental change in the Antarctic Peninsula region. *The Holocene 19,* 51-69.

Björck, Svante, 2011: personal communication. (22 Feb. 2011)

Bronk Ramsey, C., 2008: Deposition models for chronological records. *Quaternary Science Reviews* 27, 42-60.

Bronk Ramsey, C., 2009: Bayesian analysis of radiocarbon dates. *Radiocarbon 51*, 337-360.

Conley, D. J. and Schelske, C. L., 2001. Biogenic silica. In: Smol, J. P., Birks, H. J. B. & Last, W. M. (eds.): *Tracking environmental change using lake sediments; Volume 3, Terrestrial, algal, and siliceous indicators*, 281-293. Kluwer Academic Publishers, Dordrecht.

Encyclopædia Britannica Online, 2011: Trachyte. (17 Feb. 2011) http://www.britannica.com/EBchecked/topic/601494/trachyte

De Vos, B., Vandecasteele, B., Deckers, J. & Muys, B., 2005: Capability of Loss-on-Ignition as a predictor of total organic carbon in non-calcareous forest soils. *Communications in soil science and plant analysis, 36*, 2899-2921.

Fanelli, S. A.: *Ocean currents*. (21 March 2011) http://www3.ncc.edu/faculty/bio/fanellis/biosci119/currents.html

Hedin, L.-H. & Jansson, M., 2007: *Mineral i Sverige: en fälthandbok*. Björnen, Borlänge. 224 pp.

Heiri, G., Lotter, A. F. & Lemcke, G., 2001: Loss on ignition as a method for estimating organic and carbonate content in sediments: reproducibility and comparability of results. *Journal of paleolimnology 25*, 101-110.

Hess, D., 2011: *McKnight's physical geography: a landscape appreciation.* 10. ed. Prentice Hall, Boston. 554 pp.

Hodgson, D. A. & Sime, L. C., 2010: Southern westerlies and CO_2. *Nature geosciences 3,* 666-667.

Hudson, D. A. & Hewitson, B. C., 2001: The atmospheric response to a reduction in summer Ant-

arctic sea-ice axtent. *Climate research 16,* 79-99.

Jenny, B., Wilhelm, D. & Valero-Garcés, B. L., 2003: The Southern Westerlies in Central Chile: Holocene precipitation estimates based on a water balance model for Laguna Aculeo (33°50'S). *Climate Dynamics 20,* 269-280.

Lamy, F., Hebbeln, D., Röhl, U. & Wefer, G., 2001: Holocene rainfall variability in southern Chile: a marine record of latitudinal shifts of the Southern Westerlies. *Earth and planetary science letters 185,* 369-382.

Lamy, F., Kaiser, J., Arz, H. W., Hebbeln, D., Ninnemann, U., Timm, O., Timmermann, A. & Toggweiler, J. R., 2007: Modulation of the bipolar seesaw in the Southeast Pacific during Termination 1. *Earth and planetary science letters 259*, 400-413.

Lamy, F., Kilian, R., Arz, H. W., Francois, J.-P., Kaiser, J., Prange, M. & Steinke, T., 2010: Holocene changes in the position and intensity of the southern westerly wind belt. *Nature geosciences 3*, 695-699.

Ljung, Karl, 2011: personal communication. (1 March 2011)

Ljung, K., 2007: *Holocene climate and environmental dynamics on the Tristan da Cunha island group, South Atlantic.* Doctoral dissertation, Lund University. Lund. 28 pp.

Ljung, K. & Björck, S., 2007: Holocene climate and vegetation dynamics on Nightingale Island, South Atlantic – an apparent interglacial bipolar seesaw in action? *Quaternary Science Reviews 26,* 3150-3166.

Ljung, K., Björck, S., Renssen, H. & Hammarlund, D., 2008: South Atlantic Island record reveals a South Atlantic response to the 8.2 kyr event. *Climate of the Past 4,* 35-45.

Lowe, J. J. & Walker, M. J.C., 1997: *Reconstructing quaternary environments*. 2. ed. Longman, Harlow. 446 pp.

Luczak, C., Janquin, M.-A., Kupka, A., 1997: Simple standard procedure for the routine determination of organic matter in marine sediment. *Hydrobiologia 345*, 87-94.

Mayr, C., Wille, M., Haberzettl, T., Fey, M., Janssen, S., Lücke, A., Ohlendorf, C., Oliva, G., Schäbitz, Schleser, G. H. & Zolitschka, B., 2007: Holocene variability of the Southern Hemisphere westerlies in Argentinean Patagonia (52°S). *Quaternary Science Reviews 26,* 579-584.

McCormac, F. G., Hogg, A. G., Blackwell, P. G., Buck, C. E., Higham, T. F. G. & Reimer, P. J., 2004: SHCal04 Southern Hemisphere calibration, 0-11.0 cal kyr BP. *Radiocarbon 46*, 1087-1092.

Meyers, P. A. & Teranes, J. L., 2001: Sediment organic matter. In: Smol, J. P. and Last, W. M. (eds.): *Tracking environmental change using lake sediments; Volume 2, Physical and geochemical methods*, 239-269. Kluwer Academic Publishers, Dordrecht.

Moreno, P. I., Francois, J. P. & Villa-Martínez, R., 2010: Covariability of the Southern Westerlies and atmospheric CO_2 during the Holocene. *Geology 38,* 727-730.

Nielsen, S. H. H., Koç, N. & Crosta, X., 2004: Holocene climate in the Atlantic sector of the Southern Ocean: Controlled by insolation or oceanic circulation? *Geology 32,* 317-320

Ochyra, R., 1998. *The moss flora of King George Island, Antarctica.* W. Szafer Institute of Botany, Polish Academy of Sciences, Cracow. 278 pp.

Ollier, C. D., 1984: Geomorphology of South Atlantic volcanic islands. Part I: the Tristan da Cunha group. In: *Zeitschrift fur Geomorphologie 28*, 367-382.

Rasmussen, S. O., Andersen, K. K., Svensson, A. P., Steffensen, J. P., Vinther, B. M., Clausen, H. B., Siggaard-Andersen, M-L., Johnsen, S. J., Larsen, L. B., Dahl-Jensen, D., Bigler, M., Röthlisberger, R., Fischer, H., Goto-Azuma, K., Hansson, M. E. & Ruth, U., 2006: A new Greenland Ice core chronology for the last glacial Termination. *Journal of geophysical research 111*, D06102.

Reagan, M. K., Turner, S., Legg, M., Sims, K. W. W. & Hards, V. L., 2008: ^{238}U- and ^{232}Th-decay series constraints on timescales of crystal fractionation to produce the phonolite erupted in 2004 near Tristan da Cunha, South Atlantic Ocean. *Geochimica et cosmochimica acta 72*, 4367-4378.

Robinson, A., Calov, R. & Ganopolski, A., 2010: Greenland ice sheet model parameters constrained using simulations of the Eemian interglacial. *Climate of the past discussions 6*, 1551-1588.

Ryan, P. G. (ed.), 2007: *Field guide to the animals and plants of Tristan da Cunha and Gough Island.* Pisces Publications, Newbury, for the Tristan Island Government. 162 pp.

Salkind, N. J., 2008: *Statistics for people who (think they) hate statistics*. 3. ed. Sage Publications, Thousand Oaks. 405 pp.

Sandgren, P. & Snowball, I., 2001: Applications of mineral magnetic techniques to paleolimnology. In: Smol, J. P. and Last, W. M. (eds.): *Tracking environmental change using lake sediments; Volume 2, Physical and geochemical methods*, 217-237. Kluwer Academic Publishers, Dordrecht.

Talbot, M. R., 2001: Nitrogen isotopes in palaeolimnology. In: Smol, J. P. and Last, W. M. (eds.): *Tracking environmental change using lake sediments; Volume 2, Physical and geochemical methods,* 401-439. Kluwer Academic Publishers, Dordrecht.

Thomas, E. R., Wolff, E. W., Mulvaney, R., Stef-

fensen, J. P., Johnsen, S. J., Arrowsmith, C., White, J. W. C., Vaughn, B. & Popp, T., 2007: The 8.2 ka event from Greenland ice cores. *Quaternary science reviews 26,* 70-81.

Waldmann, N., Ariztegui, D., Anselmetti, F. S., Austin Jr, J. A., Moy, C., M., Stern, C., Recasens, C. & Dunbar, R. B., 2010: Holocene climatic fluctuations and positioning of the Southern Hemisphere westerlies in Tierra del Fuego (54°S), Patagonia. *Journal of quaternary science 25*, 1063-1075.

Wheater, C. P. & Cook, P. A., 2000: *Using statistics to understand the environment*. Routledge, London. 245 pp.

8 Appendix

8.1 Appendix 1

The table presents the detailed lithological description of the studied cores. UB = upper boundary, LB = lower boundary, hum fp = humified fen peat, min rich = minerogenic-rich units, gy fp = gyttja-like fen peat, si = silty, OM = organic matter

U.	Depth (cm)	Lithology	Subun. (cm)	Description
26	183-202.5	hum fp		Brown, loose, watery, very fine texture.
25	202.5-239	si gy fp		Dark brown and fine texture. Silty (sometimes sandy) and slightly lighter laminae with rather sharp boundaries, 1-5 mm wide, throughout the unit. UB = rather sharp
			202.5-212	More silty upwards, slightly lighter colour. LB = gradual
			223-224.5	Dark brown minerogenic horizon. Silty-sandy with biotite and small beige clasts of silt. UB = sharp, LB = sharp
			234.5-239	Laminae more well marked. Brown, silty, sandy, some biotite. LB = rather sharp, UB = rather sharp
24	239-250	hum fp		Very dark brown. Abundant coarse organic matter. UB = gradual
			243	Brown silty lamina, 2 mm. Clast of silt 3 mm and some smaller clasts and biotite around. LB = gradual, UB = gradual
23	250-276	si hum fp		Dark brown, some coarse OM. UB = sharp
			259.5-262	Slightly silty-sandy. LB = rather sharp, UB = gradual
22	276-286	hum fp		Very dark brown, few coarse OM. UB = sharp
21	286-311	si hum fp		Very dark brown, very few coarse OM. UB = slightly gradual
			291.7	wood fragments <14*2*2 mm
			309-311	Ca 3 beige silty laminae 1-3 mm wide. UB = sharp, LB = sharp
20	311-322	si gy fp		Dark brown, gradually coarser from medium-fine to coarse sediment upwards. UB = slightly gradual. Silty, brown laminae throughout the unit UB = sharp, LB = sharp
19	322-323.5	min rich		Very dark brown silt, sand, organic sediment and biotite. UB = rather sharp. Beige silt laminae 1-2 mm wide. UB = sharp, LB = sharp.
18	323.5-368.6	si gy fp		Very dark brown with some coarse organic matter. UB = slightly gradual
			323.5-326.5	Very dark brown, more sandy-silty upwards. LB = rather gradual
			328.3-339	Brown, peaty, abundant coarse OM. UB = gradual, LB = gradual
			346-359.5	Brown, thin, silty laminae, 1-2 mm wide. The laminations have rather sharp boundaries, the unit UB = gradual, LB = sharp
			346.5	Some coarse organic matter (in core 5) LB = rather sharp, UB = rather sharp
			351.8	Some coarse organic matter (in core 5) LB = sharp, UB = sharp
			360-362	Grey-brown silty lamina, 1 mm, at 362 cm in core 5. Coarse peat or OM above in both cores. UB = rather sharp, LB = sharp. Erosive/ outwash event?
			360.6	Wood 18*10*6 mm
			365.5-366	Brown minerogenic-rich horizon with tilted geometry. Silt, sand, organic sediment and biotite. LB = rather gradual, UB = rather gradual
			366.5-368	1-2 beige-grey silty laminae, 1 mm wide, undulating. UB = sharp, LB = sharp.
17	368.6-372	gy fp		Black, algal and very fine texture, no coarse OM. Tilted layer. UB = sharp

U.	Depth (cm)	Lithology	Subun. (cm)	Description
16	372-375.8	si hum fp		Very dark brown, high content of coarse OM. UB = sharp and tilted
			373.5	Wood 20*10*10 mm
			375.8	2 beige-grey tilted silty laminae, 1 mm wide. UB = sharp, LB = sharp
15	375.8-410	hum fp		Very dark brown, highly humified. UB = sharp
14	410-413.5	min rich		Dark brown minerogenic and organic material, some coarse OM. Less minerogenic than unit 13. UB = slightly gradual
			410-412	Brown, silty horizon. LB = Gradual, UB = slightly gradual
			412-413.5	Grey clast of silt, 20*8 mm
13	413.5-414.5	min rich		Very dark brown with beige parts and biotite. Silt, sand and organic substances. Tilted geometry. UB = gradual
12	414.5-418.5	hum fp		Dark brown with coarse organic matter. UB = sharp
			415.5-417.5	Beige clast of silt 25*10 mm
			416-417.5	Abundant coarse organic matter. UB = slightly gradual, LB = slightly gradual
			417	wood 14*2*2 mm
11	418.5-422	hum fp		Dark brown, highly humified, few coarse organic matter. UB = rather sharp
10	422-469	hum fp		Very dark brown with few coarse OM. Slightly silty. UB = slightly gradual
			422.5	Wood piece 10*2*2 mm
			448	Shell fragments or other macrofossil <4 mm
			460-469	Very abundant coarse OM. UB = gradual
			468	Wood pieces <10*4*4 mm
9	469-472	hum fp		Very dark brown, highly humified, few coarse organic matter. UB = gradual
8	472-483	hum fp		Very dark brown sediment with dark brown laminae. Some coarse OM. UB = rather sharp
			472-482	ca. 5 dark brown laminae, silty, 3-10 mm wide. UB = sharp, LB = sharp
			477.5	wood 13*3*3 mm
7	483-484.5	min rich		Brown, dark brown, beige silty-sandy, organic substances and biotite. Small silty conglomerates. Undulating geometry. UB = rather sharp
			483-484	Beige-grey clast of silt, 15 mm
			483.3	Pebble of trachyte, 7*5*5 mm
6	484.5-498.8	gy fp		Black-brown, softer in the bottom, more compact up to 484 cm. Some small coarse OM. UB = rather sharp
			483.5-491	Higher minerogenic content, silty sandy upwards, some biotite. Black-brown with small (mm) beige clasts of silt. LB = gradual, UB = rather sharp
			485	Slightly sandy
			490.6-491.4	Grey clast of silt, 10*8 mm
5	498.8-508	hum fp		Dark brown peat, a few coarse OM. Softer and more watery upwards. UB = rather sharp
4	508-531	hum fp		Dark brown, highly humified, few coarse organic matter. UB = gradual
			527	Piece of wood or root 6 mm and a large piece of wood, 24*11*12 mm
3	531-534	min rich		Very dark brown silt and fine-grained sediment, some sand, organic substances and biotite. Tilted geometry. UB = rather sharp
			532-533.3	Beige clast of silt, 20*9 mm

U.	Depth (cm)	Lithology	Subun. (cm)	Description
2	534-539	hum fp		Dark brown, some coarse OM. UB = slightly gradual
1	539-668	highly hum fp		Very dark brown, compact, slightly algal-rich and very fine textured sediment. UB = slightly gradual. Core 1 more compact than core 2. Coarser OM seem to be present every here and there throughout the unit.
			577-578.5	Beige clast of silt, 30*15 mm. Unevenly wide, undulating boundaries, core 2.
			583	Grey clast of silt, 15*9 mm, in core 2.
			588-589.5	Beige clast of silt, 40*20 mm. Unevenly wide, undulating boundaries, core 1.
			596-605	Several beige clasts of silt, 1-4 mm, in core 1.
			605	Beige clast of silt, 20*1 mm wide in core 1.
			607-608	Very dark brown, probably macrofossil fragments. UB = sharp, LB = sharp
			621-622.5	Very dark brown, some pieces of macrofossils and a few beige clasts of silt (1-3 mm). UB = sharp, LB = sharp
			639-643	Coarse OM, most likely wood fragments. Slightly lighter very dark brown. UB = sharp, LB = sharp

8.2 Appendix 2

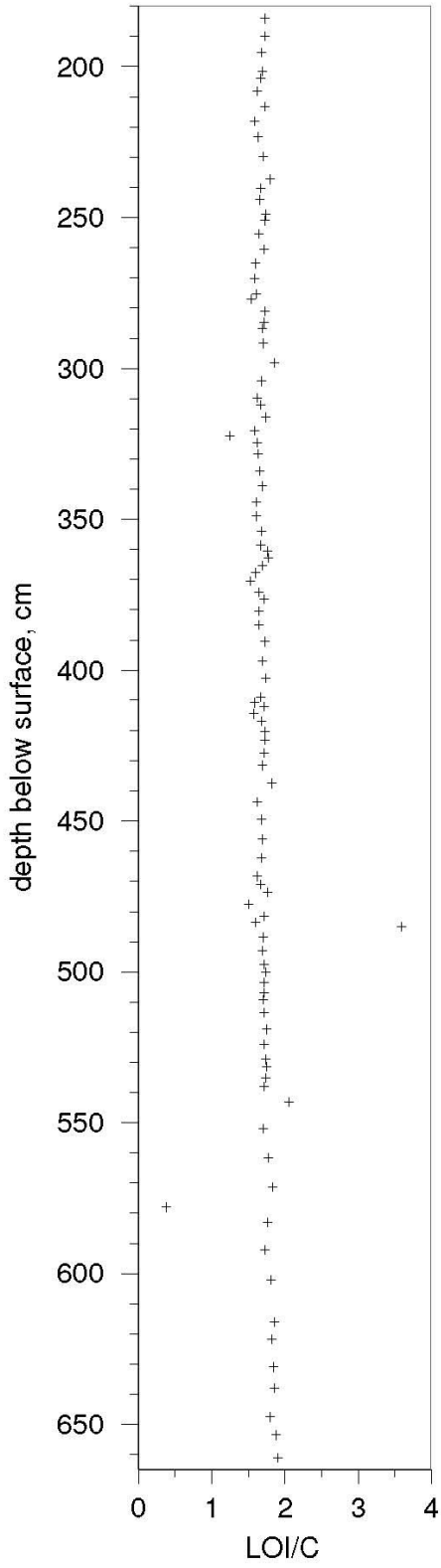

The graph shows the LOI/TC ratio. Average value is 1.70.
SE = 0.02 and 2SD = 0.49.

Tidigare skrifter i serien ”Examensarbeten i Geologi vid Lunds Universitet”:

227. Mehlqvist, Kristina, 2008: En mellanjurassisk flora från Bagå-formationen, Bornholm. (15 hskp)
228. Lindvall, Hanna, 2008: Kortvariga effekter av tefranedfall i lakustrin och terrestrisk miljö. (15 hskp)
229. Löfroth, Elin, 2008: Are solar activity and cosmic rays important factors behind climate change? (15 hskp)
230. Damberg, Lisa, 2008: Pyrit som källa för spårämnen – kalkstenar från övre och mellersta Danien, Skåne. (15 hskp)
331. Cegrell, Miriam & Mårtensson, Jimmy, 2008: Resistivity and IP measurements at the Bolmen Tunnel and Ådalsbanan, Sweden. (30 hskp)
232. Vang, Ina, 2008: Skarn minerals and geological structures at Kalkheia, Kristiansand, southern Norway. (15 hskp)
233. Arvidsson, Kristina, 2008: Vegetationen i Skandinavien under Eem och Weichsel samt fallstudie i submoräna organiska avlagringar från Nybygget, Småland. (15 hskp)
234. Persson, Jonas, 2008: An environmental magnetic study of a marine sediment core from Disko Bugt, West Greenland: implications for ocean current variability. (30 hskp)
235. Holm, Sanna, 2008: Titanium- and chromium-rich opaque minerals in condensed sediments: chondritic, lunar and terrestrial origins. (30 hskp)
236. Bohlin, Erik & Landen, Ludvig, 2008: Geofysiska mätmetoder för prospektering till ballastmaterial. (30 hskp)
237. Brodén, Olof, 2008: Primär och sekundär migration av hydrokarboner. (15 hskp)
238. Bergman, Bo, 2009: Geofysiska analyser (stångslingram, CVES och IP) av lagerföljd och lakvattenrörelser vid Albäcksdeponin, Trelleborg. (30 hskp)
239. Mehlqvist, Kristina, 2009: The spore record of early land plants from upper Silurian strata in Klinta 1 well, Skåne, Sweden. (45 hskp)
239. Mehlqvist, Kristina, 2009: The spore record of early land plants from upper Silurian strata in Klinta 1 well, Skåne, Sweden. (45 hskp)
240. Bjärnborg, Karolina, 2009: The copper sulphide mineralization of the Zinkgruvan deposit, Bergslagen, Sweden. (45 hskp)
241. Stenberg, Li, 2009: Historiska kartor som hjälp vid jordartsgeologisk kartering – en pilotstudie från Vångs by i Blekinge. (15 hskp)
242. Nilsson, Mimmi, 2009: Robust U-Pb baddeleyite ages of mafic dykes and intrusions in southern West Greenland: constraints on the coherency of crustal blocks of the North Atlantic Craton. (30 hskp)
243. Hult, Elin, 2009: Oligocene to middle Miocene sediments from ODP leg 159, site 959 offshore Ivory Coast, equatorial West Africa. (15 hskp)
244. Olsson, Håkan, 2009: Climate archives and the Late Ordovician Boda Event. (15 hskp)
245. Wollein Waldetoft, Kristofer, 2009: Svekofennisk granit från olika metamorfa miljöer. (15 hskp)
246. Månsby, Urban, 2009: Late Cretaceous coprolites from the Kristianstad Basin, southern Sweden. (15 hskp)
247. MacGimpsey, I., 2008: Petroleum Geology of the Barents Sea. (15 hskp)
248. Jäckel, O., 2009: Comparison between two sediment X-ray Fluorescence records of the Late Holocene from Disko Bugt, West Greenland; Paleoclimatic and methodological implications. (45 hskp)
249. Andersen, Christine, 2009: The mineral composition of the Burkland Cu-sulphide deposit at Zinkgruvan, Sweden – a supplementary study. (15 hskp)
250. Riebe, My, 2009: Spinel group minerals in carbonaceous and ordinary chondrites. (15 hskp)
251. Nilsson, Filip, 2009: Föroreningsspridning och geologi vid Filborna i Helsingborg. (30 hskp)
252. Peetz, Romina, 2009: A geochemical characterization of the lower part of the Miocene shield-building lavas on Gran Canaria. (45 hskp)
253. Åkesson, Maria, 2010: Mass movements as contamination carriers in surface water systems – Swedish experiences and risks.
254. Löfroth, Elin, 2010: A Greenland ice core perspective on the dating of the Late

Bronze Age Santorini eruption. (45 hskp)

255. Ellingsgaard, Óluva, 2009: Formation Evaluation of Interlava Volcaniclastic Rocks from the Faroe Islands and the Faroe-Shetland Basin. (45 hskp)
256. Arvidsson, Kristina, 2010: Geophysical and hydrogeological survey in a part of the Nhandugue River valley, Gorongosa National Park, Mozambique. (45 hskp)
257. Gren, Johan, 2010: Osteo-histology of Mesozoic marine tetrapods – implications for longevity, growth strategies and growth rates. (15 hskp)
258. Syversen, Fredrikke, 2010: Late Jurassic deposits in the Troll field. (15 hskp)
259. Andersson, Pontus, 2010: Hydrogeological investigation for the PEGASUS project, southern Skåne, Sweden. (30 hskp)
260. Noor, Amir, 2010: Upper Ordovician through lowermost Silurian stratigraphy and facies of the Borenshult-1 core, Östergötland, Sweden. (45 hskp)
261. Lewerentz, Alexander, 2010: On the occurrence of baddeleyite in zircon in silica-saturated rocks. (15 hskp)
262. Eriksson, Magnus, 2010: The Ordovician Orthoceratite Limestone and the Blommiga Bladet hardground complex at Horns Udde, Öland. (15 hskp)
263. Lindskog, Anders, 2010: From red to grey and back again: A detailed study of the lower Kundan (Middle Ordovician) 'Täljsten' interval and its enclosing strata in Västergötland, Sweden. (15 hskp)
264. Rääf, Rebecka, 2010: Changes in beyrichiid ostracode faunas during the Late Silurian Lau Event on Gotland, Sweden. (30 hskp)
265. Petersson, Andreas, 2010: Zircon U-Pb, Hf and O isotope constraints on the growth versus recycling of continental crust in the Grenville orogen, Ohio, USA. (45 hskp)
266. Stenberg, Li, 2010: Geophysical and hydrogeological survey in a part of the Nhandugue River valley, Gorongosa National Park, Mozambique – Area 1 and 2. (45 hskp)
267. Andersen, Christine, 2010: Controls of seafloor depth on hydrothermal vent temperatures - prediction, observation & 2D finite element modeling. (45 hskp)
268. März, Nadine, 2010: When did the Kalahari craton form? Constraints from baddeleyite U-Pb geochronology and geo-chemistry of mafic intrusions in the Kaapvaal and Zimbabwe cratons. (45 hskp)
269. Dyck, Brendan, 2010: Metamorphic rocks in a section across a Svecnorwegian eclogite-bearing deformation zone in Halland: characteristics and regional context. (15 hskp)
270. McGimpsey, Ian, 2010: Petrology and lithogeochemistry of the host rocks to the Nautanen Cu-Au deposit, Gällivare area, northern Sweden. (45 hskp)
271. Ulmius, Jan, 2010: Microspherules from the lowermost Ordovician in Scania, Sweden – affinity and taphonomy. (15 hskp)
272. Andersson, Josefin, Hybertsen, Frida, 2010: Geologi i Helsingborgs kommun – en geoturistkarta med beskrivning. (15 hskp)
273. Barth, Kilian, 2011:Late Weichselian glacial and geomorphological reconstruction of South-Western Scania, Sweden. (45 hskp)
274. Mashramah, Yaser, 2011: Maturity of kerogen, petroleum generation and the application of fossils and organic matter for paleotemperature measurements. (45 hskp)
275. Vang, Ina, 2011: Amphibolites, structures and metamorphism on Flekkerøy, south Norway. (45 hskp)
276. Lindvall, Hanna, 2011: A multi-proxy study of a Holocene peat sequence on Nightingale Island, South Atlantic. (45 hskp)
277. Bjerg, Benjamin, 2011: Metodik för att förhindra metanemissioner från avfallsdeponier, tillämpad vid Albäcksdeponin, Trelleborg. (30 hskp)

LUNDS UNIVERSITET

Geologiska enheten
Institutionen för geo- och ekosystemvetenskaper
Sölvegatan 12, 223 62 Lund